ANTENNA BEAMFORMING USING OPTICAL PROCESSING

L.P. Anderson, F. Boldissar, D.C.D. Chang

Hughes Aircraft Company
Space and Communiations Group
Technology Division
Antenna Systems Laboratory
El Segundo, California

Prepared For
National Aeronautics and Space Administration

NASA Lewis Research Center
Contract NAS3-24889

ASDR:MD87-2/090:bjl

1. Report No.	2. Government Accession No.	3. Recipient's Catalog No.
CR-180844		

4. Title and Subtitle	5. Report Date
ANTENNA BEAMFORMING USING OPTICAL PROCESSING	JUNE 1987
	6. Performing Organization Code

7. Author(s)	8. Performing Organization Report No.
L.P. ANDERSON, JR. F. BOLDISSAR DCD CHANG	10. Work Unit No.

9. Performing Organization Name and Address	11. Contract or Grant No.
HUGHES AIRCRAFT CO. SPACE & COMMUNICATIONS GROUP TECHNOLOGY DIVISION EL SEGUNDO, CALIFORNIA 90245	NAS 3-24889
	13. Type of Report and Period Covered
	CONTRACTOR REPORT

12. Sponsoring Agency Name and Address	14. Sponsoring Agency Code
NATIONAL AERONAUTICS AND SPACE ADMINISTRATION WASHINGTON, D.C. 20546	

15. Supplementary Notes

PROJECT MANAGER, RICHARD KUNATH
SPACE COMMUNICATIONS DIVISION
NASA - LEWIS RESEARCH CENTER
CLEVELAND, OHIO

16. Abstract

This work concerns itself with the analytical investigation into the feasibility of optical processor based beamforming for microwave array antennas. The primary focus is on systems utilizing the 20/30 GHz communications band and a transmit configuration exclusively to serve this band.

A mathematical model is developed for computation of candidate design configurations. The model is capable of determination of the necessary design parameters required for both spatial aspects of the microwave "footprint" (beam) formation as well as transmitted signal quality. Computed example beams transmitted from geosynchronous orbit are presented to demonstrate network capabilities. A comprehensive device/component survey is also conducted in parallel to determine the feasibility of breadboarding a transmit processor. Recommendations are made for the configuration of such a processor and the components which would comprise such a network.

17. Key Words (Suggested by Author(s))	18. Distribution Statement
OPTICAL BEAMFORMING NETWORK (O.B.F.N.) SPATIAL LIGHT MODULATOR (S.L.M.) FOURIER TRANSFORM LENS (F.T.L.)	UNCLASSIFIED - UNLIMITED

19. Security Classif. (of this report)	20. Security Classif. (of this page)	21. No. of pages	22. Price*
UNCLASSIFIED	UNCLASSIFIED	65	

*For sale by the National Technical Information Service, Springfield, Virginia 22161

TABLE OF CONTENTS

LIST OF FIGURES

LIST OF TABLES

EXECUTIVE SUMMARY

This work concerns itself with the analytical investigation into the feasibility of optical processor based beamforming for microwave array antennas. The primary focus is on systems utilizing the 20/30 GHz communications band and a transmit configuration exclusively to serve this band.

A mathematical model is developed for computation of candidate design configurations. The model is capable of determination of the necesarry design parameters required for both spatial aspects of the microwave "footprint" (beam) formation as well as transmitted signal quality. Computed example beams transmitted from geosynchronous orbit are presented to demonstrate network capabilities. A comprehensive device/component survey is also conducted in parallel to determine the feasibility of breadboarding a transmit processor. Recommendations are made for the configuration of such a processor and the components which would comprise such a network.

Concluding remarks outline a suggested direction for future studies to occur. This includes areas to be addressed for the refinement of the analytical model as well as aspects of needed device development to realize such networks.

INTRODUCTION

This report documents the initial phase of a feasibility study to investigate optical processor based antenna beamforming networks. Keopf[1] has described the basic concept for both transmit and receive applications. In his description, a heterodyne processing scheme is used in conjunction with a static means (i.e. pinhole mask) for production of a scaled image of the desired far field pattern.

The scope of this effort was to derive a transmit architecture which would be tractable to formation of generalized shaped beam far field patterns. Thus a dynamic means for image formation must be employed. Additionally, the system should be capable of operation in the 20/30 GHz communications band. These requirements necessitated consideration of alternative approaches due to inherent limitations in the Keopf method in addressing these requirements. Once this basic processor configuration was established, a computer model of the network was generated for analysis of its beamforming capabilities from both spatial and temporal aspects. Specifically, the quality of the processor formed far field footprint (e.g. resolution, gain-area product, sidelobe levels, etc.) as well as the transmitted signal quality at the output of the processor (e.g. S/N ratio, noise figure, etc.) was quantitatively examined in order to establish processor performance.

---

1. G.A. Keopf "Optical Processor for Phased Array Antenna Beam Formation" SPIE Vol. 477 1984

The creation of such a model serves a twofold purpose. First, it allows the user to quantitatively evaluate various processor designs for their performance characteristics. Second, and most importantly, it allows the user to define the specification of key components based on performance requirements delineated by spatial and temporal qualities of the transmit beam. For example, the spatial characteristics (i.e. radiation pattern) of the far field footprint is directly affected by the design of the spatial light modulator used for image formation.

To date no attempt has been made to model the effects of the spatial image forming path as applied to antenna beamforming, albeit this approach has been addresed from the more generalized vein of Fourier transform based processors[2,3]. Aspects of the temporal characteristics of the network have been addressed in previous works[4,5] some results of which have been incorporated in the model. The evaluation of network power efficiency though, is unique to this project.

The eventual goal of these studies is to establish a structured approach to the design and build of optical processor based beamforming networks. This includes recommendations for specific component configurations as applied to specialized

---

2. Kingston, et al "Fourier Transformation Using an Electro-Absorbtive CCD Spatial Light Modulator" IEEE Journal of QE QE-19 No. 9 9/83
3. Casasent, et al "Phase Error Model for Simple Fourier Transform Lenses" Applied Optics Vol. 17 No. 11 6/78
4. Stephens, et al "System Characteristics of Direct Modulated and Externally Modulated RF Fiber Optic Links" IEEE Journal of LT. LT 5 #3 3/87
5. HAC/HRL "Millimeter Wave/Fiber Optic Links" HRL Technical Report Vol. I. Proposal No. 84M-0109/F6118 (RADC) Jan. 1984

requirements. For example, the surface of the spatial light modulator can be defined for a specific field of view and resolution accuracy (e.g. CONUS coverage. CONUS is an acronym for Continental United States).

This work was conducted for the NASA-Lewis Research Center Applications Notice Program (Contract Number NAS 3-24889).

1.0 NETWORK CONSIDERATION

The scope of this study concerned itself with the analysis of a transmit optical processor based beamforming network. Thus, a discussion of the feasibility of receive networks based on the optical processor concept are not addressed herein.

Initially, two architectures were studied for their relative qualitative merits before the development of the analysis model. Several key factors were deemed common to the evaluation of network performance in each case. Here, potential application to communications platforms using the 20/30 GHz band is critical. Both architectures are based on the Fourier transform relationship between the front and rear focal planes of an optical lens[6]. Recognizing the fact that the far field distribution of a planar array is approximately the Fourier transform of its aperture distribution, the complex excitation of the array aperture can be achieved by the scaled optical generation of the desired pattern in the rear focal plane of the optical lens. The optical Fourier transformed output of the lens is then sampled by an array of fiber optic transmission lines, each of which transmit the spatial frequency distribution to the antenna array aperture. It is at the array aperture that these signals are downconverted (via photodetectors) and amplified for radiation at microwave frequencies. Since these photodetectors are square law devices, the phase component of the complex distribution can only be detected by superimposing a phase reference beam at the fiber interface. The frequency of the reference beam is offset by the desired microwave information signal. Thus each photodetector generates a current oscillating at the microwave frequency apparent from the inteference of the two beams. Here, both amplitude

---

6. J.W. Goodman Introduction to Fourier Optics Chapter 5 page 87

and phase information imparted to the antenna aperture from the processor is maintained.

The two architectures are depicted in Figures 1.1, 1.2. The method in Figure 1.1 is based on the microwave information signal being contained in a frequency offset between two coherent (laser) sources. These beams can be created either acousto optically or by use of two separate sources. Acousto optic generation is based on the Bragg effect. Here, an acoustic wave of frequency $\tilde{a}$ propagating through an acousto-optic material produces a travelling index grating which effects an incident optical wave of frequency ω_o. The diffracted wave is shifted in frequency $\omega_d = \omega_o \pm \omega_a$. Proper alignment of the device with the incident optical wave wil create a single sideband modulation, more commonly known as the first order beam. A potential problem though, is that physical limitations of acousto optic materials constrain modulating frequencies to an upper limit of approximately 1-2 GHz[7]. This limitation eliminates this scheme from potential 20/30 GHz applications. The utilization of two sources to generate the microwave output in a heterodyne scheme has also been considered. A fundamental limitation in this approach though is the requirement of phase coherence between the two sources. Here, a phase locked loop must be implemented to achieve this goal. An additional requirement of very narrow linewidths from the source must be available (on the order of kHz) before the phase locked loop scheme is practical. Due to these difficulties, it was decided to study the single source scheme with the microwave frequency furnished via external modulation. This

7. T. Tamir Integrated optics Topics in Applied Physics Vol. 7 Springer-Verlag 1975.

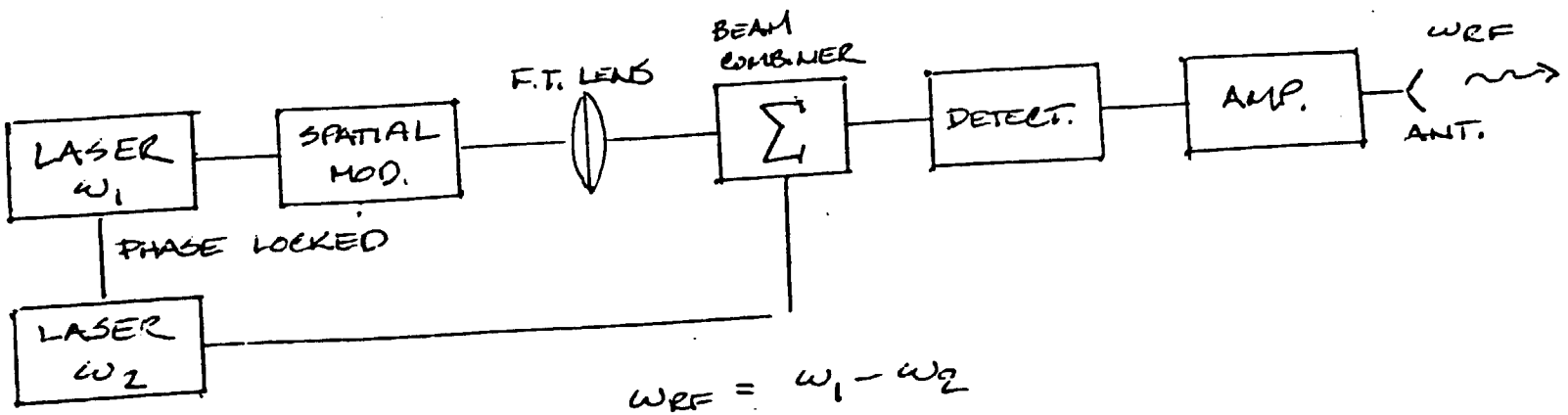

FIGURE 1.1 DUAL SOURCE HETERODYNE OPTIAL PROCESSOR BFN

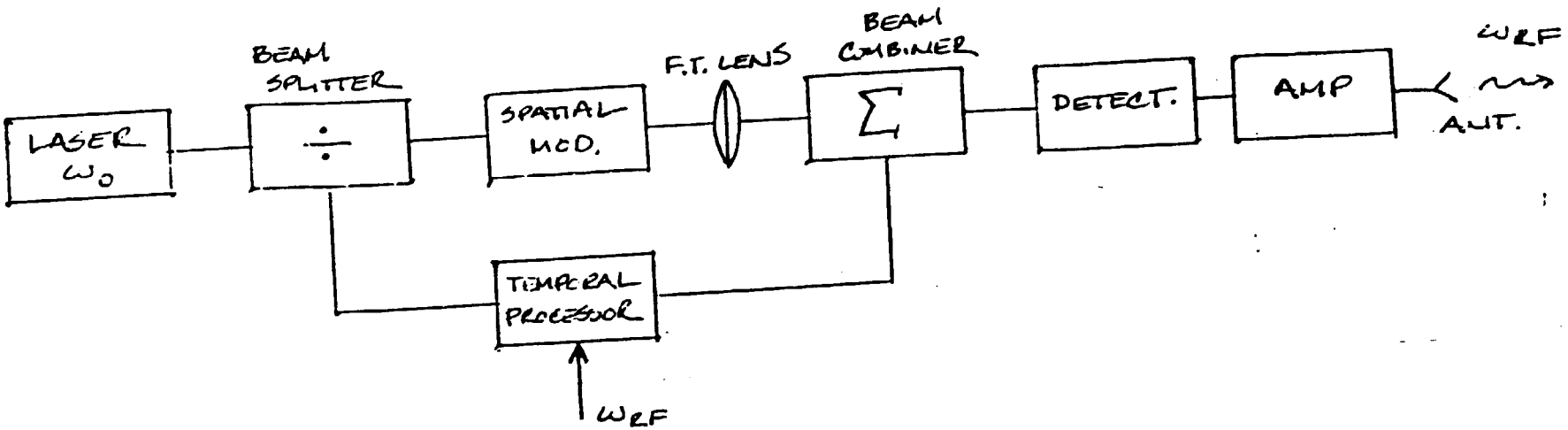

FIGURE 1.2 SINGLE SOURCE HETERODYNE OPTICAL PROCESSOR BFN

scheme has the advantage that off the shelf semiconductor lasers can be utilized as the coherent source. This scheme also has the advantage of coherent detection. In this manner, the stringent requirements of narrow source linewidths is relaxed. Here the response of the optical devices used in the network (e.g. light valves, detectors) determine the maximum acceptable linewidth of the source. Current state of the art devices exhibit frequency stability on the order of MHz. This should be more than sufficient for the envisioned applications. The projected power requirements (addressed in detail in Section 3.0) can be achieved using recent advances[8] in laser diode array techniques.

An additional point is consideration of the chosen operating wavelength of 1.3μm. This choice was based on (1) fiber losses being minimum at this wavelength and (2) optical damage in $LiNbO_3$ E/O modulators is minimized. The primary difficulty with the chosen concept though is the existance of a spatial light modulator (i.e. light valve) which operates at this wavelength. Current liquid crystal based light valves operate at .65-.45μm ranges. Discussions with design personnel at Hughes facilities have revealed that a low risk, four to six month development program should yield a device which operates at the desired wavelength.

A particular item of interest in the proposed system is the utilization of an amplitude modulation scheme in the temporal path of the processor. Here, an external electro-optic modulator provides the microwave frequency difference

8. For example see "Injection Phase Locked Laser Diode Array" NASA Tech Briefs April 1987

detected when both spatial and temporal paths are superimposed and detected. In this manner both phase and amplitude characteristics of the microwave aperture distribution is preserved at the processor output.

It is a well known fact that when the optical carrier is convolved with an amplitude modulating signal, double sidebands result. This particular aspect of the modulation format as applied to the processor operation has a severe impact on phase scanned beams. As shown in Appendix A, once the down conversion process is accomplished, a "negative angle" beam is formed for beams scanned off boresight. To eliminate the formation of such beams, this utilization of an optical circuit similar to those used for single sideband modulation in the temporal domain was considered. Here a phase quadrature signal is generated in a semi-active integrated optical circuit depicted in Figure 1.3. The input optical carrier, generated at the source, is operated on in parallel to achieve both carrier suppression and elimination of the negative angle beam formation. The development of the formulation allows for a random phase difference between the optical carrier and the applied microwave modulating signal. The resultant down converted signal upon square law detection yields the desired distribution with the aperture phase preserved. Note that the module contains both electroptic modulators and optical phase shifters to achieve this task. The effect of phase shifter errors on signal purity at detection remains to be a subject for further study.

2.0 SPATIAL ANALYSIS

The spatial path of the network is shown as Path B in Figure 2.1. Tracking the laser beam through the network, we see that the beam is first expanded and collimated with a pin-hole aperture and a lens to approximate a plane wave. The

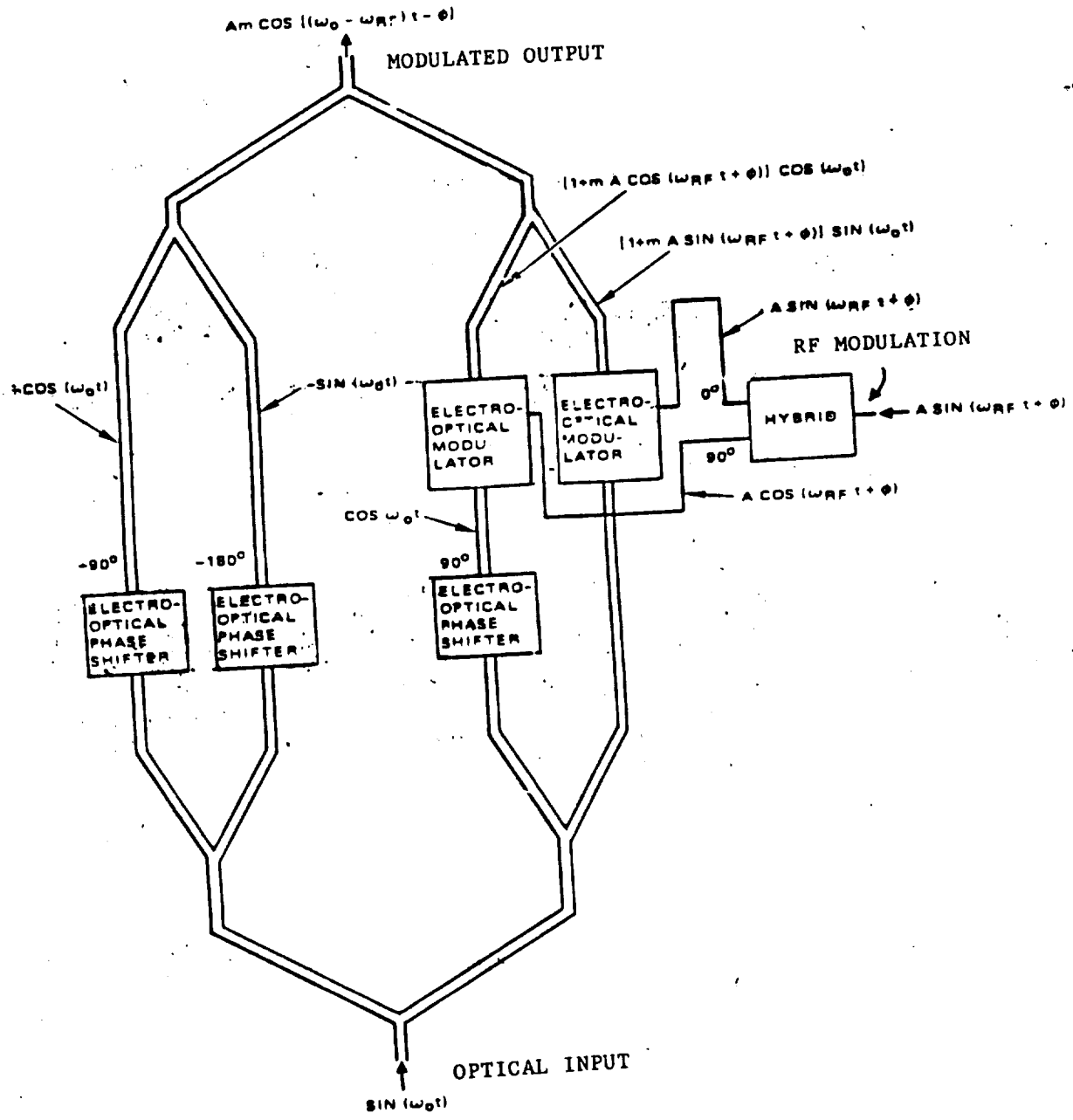

FIGURE 1.3 TEMPORAL PROCESSOR MODULE

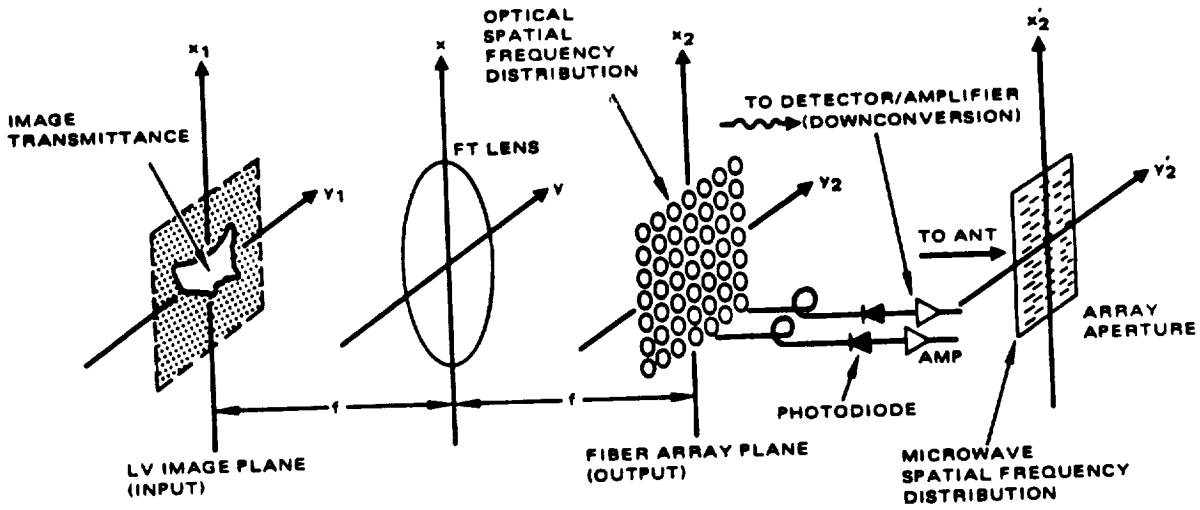

FIGURE 2.1 SPATIAL PROCESSING PATH FOR ANTENNA BEAM FORMING

plane wave is then imaged onto a spatial light modulator. The modulator, which can operate in the transmitted or reflected mode, generally consists of an electronically addressable liquid crystal display sandwiched between a pair of crossed polarizers. It is sometimes referred to as a liquid crystal light valve (LCLV). If this electrode configuration on the LCLV is a matrix of pixels, a variety of different transmittance functions can be impressed on the beam, with each transmittance function corresponding to a different antenna beam shape. The LCLV is located in the forward focal plane of a lens producing a Fourier transform of the light valve image in the rear focal plane. It is in the latter plane that the beam is optically mixed with the temporal path signal and discretly sampled by an array of optical fibers, one fiber for each antenna elment. A micro-lens array may or may not be used to facilitate power transfer into the fibers. The fibers are connected to high-speed photodetectors where the optical signals are downconverted to RF, amplified and reradiated by the antenna elements.

A computer program was developed to model the main components of the spatial arm of the BFN, namely the LCLV, the Fourier transform (FT) lens, the discrete sampling by the individual optical fibers and the resultant antenna pattern produced by the network. Refer to Appendix C for a complete description of the code. A monochromatic (optical) uniform plane wave is assumed to impinge the LCLV so that the complex electronic field exciting the light valve is given by[9]:

$$E(x_1, y_1) = t(x_1, y_1) E_o \qquad (2.0.1)$$

where E_o = input field to the LCLV

9. Goodman, op. cit.

and t = LCLV transmittance function

After passing through the FT lens, the field at the fiber array is given by[10]

$$E(x_2,y_2) = \frac{E_o}{j\lambda_o f} \iint_{-\infty}^{+\infty} t(x_1, y_1)\, P(x_1+x_2, y_1+y_2)$$

$$\text{x} \exp\left[-j\frac{2\pi}{\lambda_o f}(x_1x_2 + y_1y_2)\right] dx_1 dy_1$$

where λ_o = optical wavelength

f = FT lens focal length

and

P = lens pupil function

If the lens is large enough, P→1, which we will assume. We will also assume the LCLV electrode configuration to be a matrix of square pixels, each of size a x a, and each with a constant transmittance over its area. Thus, for a single pixel with its center at the origin,

$$t(x_1,y_1) = \begin{cases} t_o & \left(\frac{-a}{2} \le x_1 \le \frac{a}{2};\ \frac{-a}{2} \le y_1 \le \frac{a}{2}\right) \\ 0 & \text{(otherwise)} \end{cases}$$

and $$E(x_2,y_2) = \frac{E_o}{j\lambda_o f}\left\{t_o a^2 \operatorname{sinc}(af_x)\ \operatorname{sinc}(af_y)\right\}$$

where $f_x = \frac{x_2}{\lambda_o f}$ (spatial frequency in x-direction)

$f_y = \frac{y_2}{\lambda_o f}$ (spatial frequency in y-direction)

---

10. Ibid

and $\text{sinc}(z) = \frac{\sin \pi z}{\pi z}$

If the pixel is offset along the x_1 - axis by a distance b, a phase term is introduced:

$$E(x_2,y_2) = \frac{E_o}{j\lambda_o f}\left\{t_o a^2 \text{ sinc } (af_x) \text{ sinc } (af_y)\right\} e^{-j2\pi bf_x} \qquad (2.0.4)$$

Extending this idea to an N x M matrix of pixels reduces the FT integral to a double summation:

$$E(x_2,y_2) = \frac{E_o}{j\lambda_o f} \sum_{n=1}^{N} \sum_{m=1}^{M} \left\{ t_{m,n}\, a^2 \text{ sinc}(af_x) \text{ sinc}(af_y) \right.$$

$$\left. x\exp\left(-j\, 2\pi\, (b_m f_x + c_n f_y)\right)\right\} \qquad (2.0.5)$$

where $t_{m,n}$ = transmittance of the m,nth pixel

b_m = offset of the $t_{m,n}$ pixel in the x_1 -direction

and c_n = offset of the $t_{m,n}$ pixel in the y_1 -direction

The amplitude and phase of $E(x_2,y_2)$ is computed by the model at each optical fiber location, and since each fiber is attached to an antenna array element, this distribution is used to compute the antenna pattern of the array via standard aperture field techniques (i.e. physical optics).

After the computer program was developed to analyze the BFN, some design guidelines were necessary to specify the LCLV and fiber array parameters. First, the antenna array geometry is assumed. Specifying the maximum scan angle, θ_{scan}, allows light valve and fiber array sizes to be related to the antenna array size (refer to Figure 2.2) by equating maximum phase shift at the edge of both arrays:

$$\left.\begin{aligned} \frac{x_1 D_{fib}}{\lambda_{of}} &= \frac{D_{array}}{\lambda_m} \sin\theta_{scan} \\ \lambda_m &\equiv \text{microwave wavelength} \end{aligned}\right\} \qquad (2.0.1)$$

Another useful equation relates the illuminated pixel-packet size, A_{pix}, to the portion of the illuminated antenna array, A_{array}:

$$A_{array} = \frac{2\lambda_{of}}{A_{pix}} \left[\frac{D_{array}}{D_{fib}}\right] \qquad (2.0.8)$$

For a given antenna array geometry, these expressions along with the physical size limitations of the components allow the BFN designs to specify the LCLV and fiber array sizes and compute which pixels of the light valve must be "on" to produce a desired antenna contour beam.

The computer model was used to perform a case study to calculate antenna coverage beams from given LCLV inputs. A baseline geosynchronous orbital slot of 71°W was assumed along with an appropriate antenna array (Table 2.1.1 lists the antenna array parameters). Using the above expressions, a light valve was designed to excite the array to produce CONUS coverage, mid-west US coverage (roughly ¼ CONUS) and multiple spot coverage using the same BFN. The pixel arrangement of the LCLV is shown in Figure 2.3. The calculated antenna patterns, shown in Figures 2.4, 2.5, and 2.6, agree reasonably well with the light valve inputs used to generate them. These calculations were done assuming an

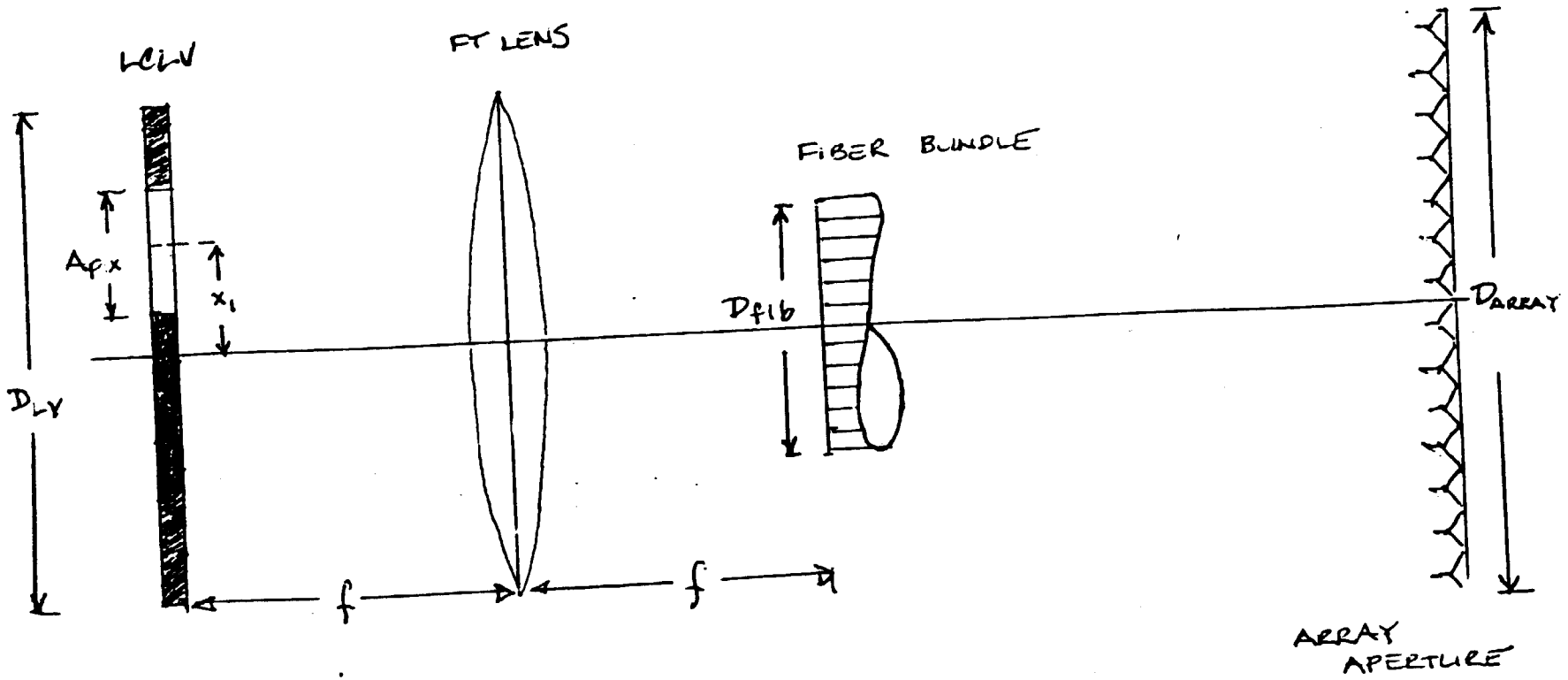

FIGURE 2.2 PROCESSOR GEOMETRY FOR BEAM SCALING

TABLE 2.1.1

MICROWAVE ANTENNA ARRAY PARAMETERS

TYPE:	PLANAR ARRAY (SQUARE)
ELEMENT:	UNIFORMLY ILLUMINATED SQUARE MODULES
NO. OF ELEMENTS:	121
SIZE:	79 λ_m
FREQUENCY:	20 GHz
PEAK GAIN:	49 dB

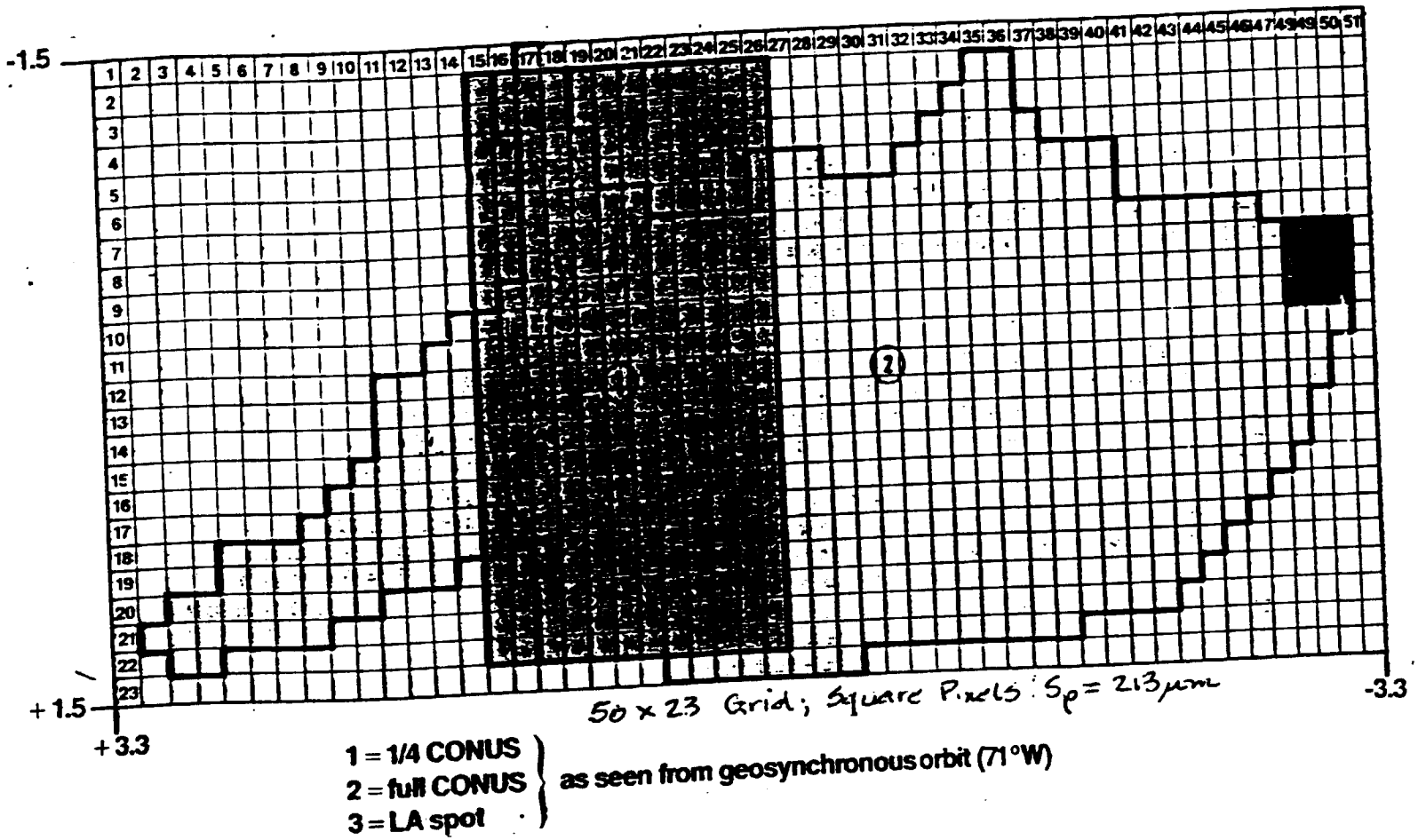

FIGURE 2.3 LIQUID CRYSTAL LIGHT VALVE MODEL

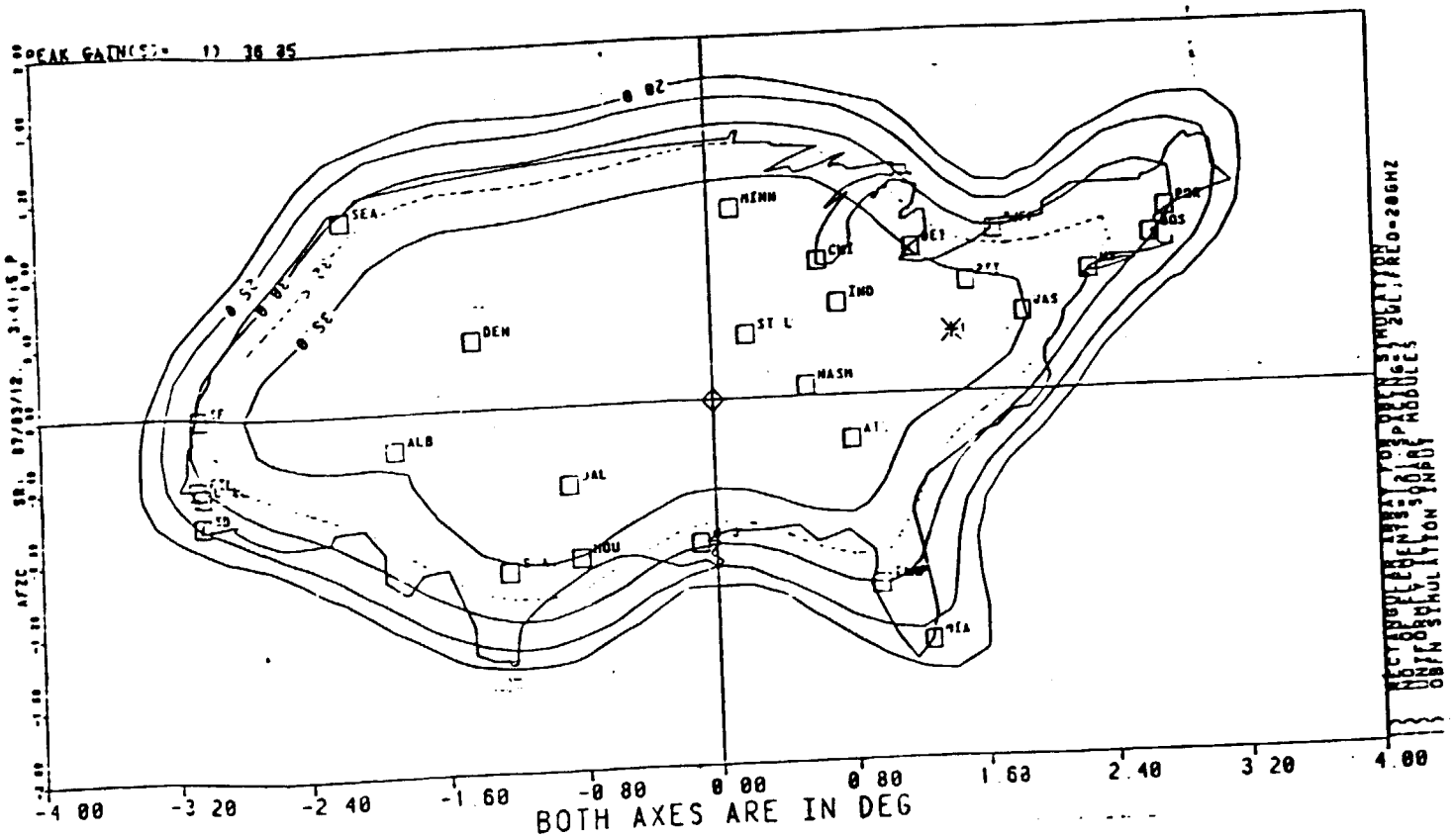

FIGURE 2.4 FULL CONUS BEAM

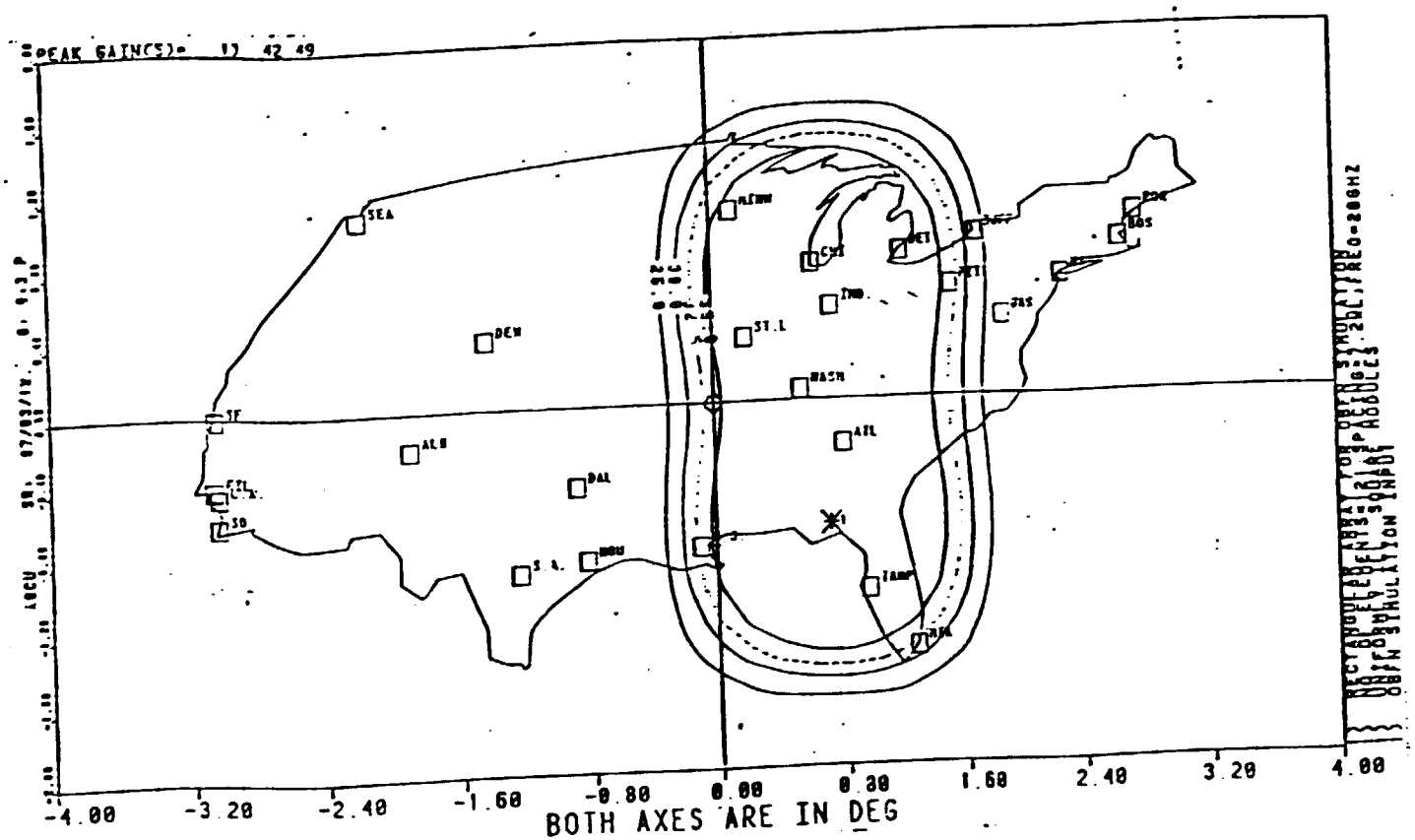

FIGURE 2.5 QUARTER CONUS BEAM (MIDWEST)

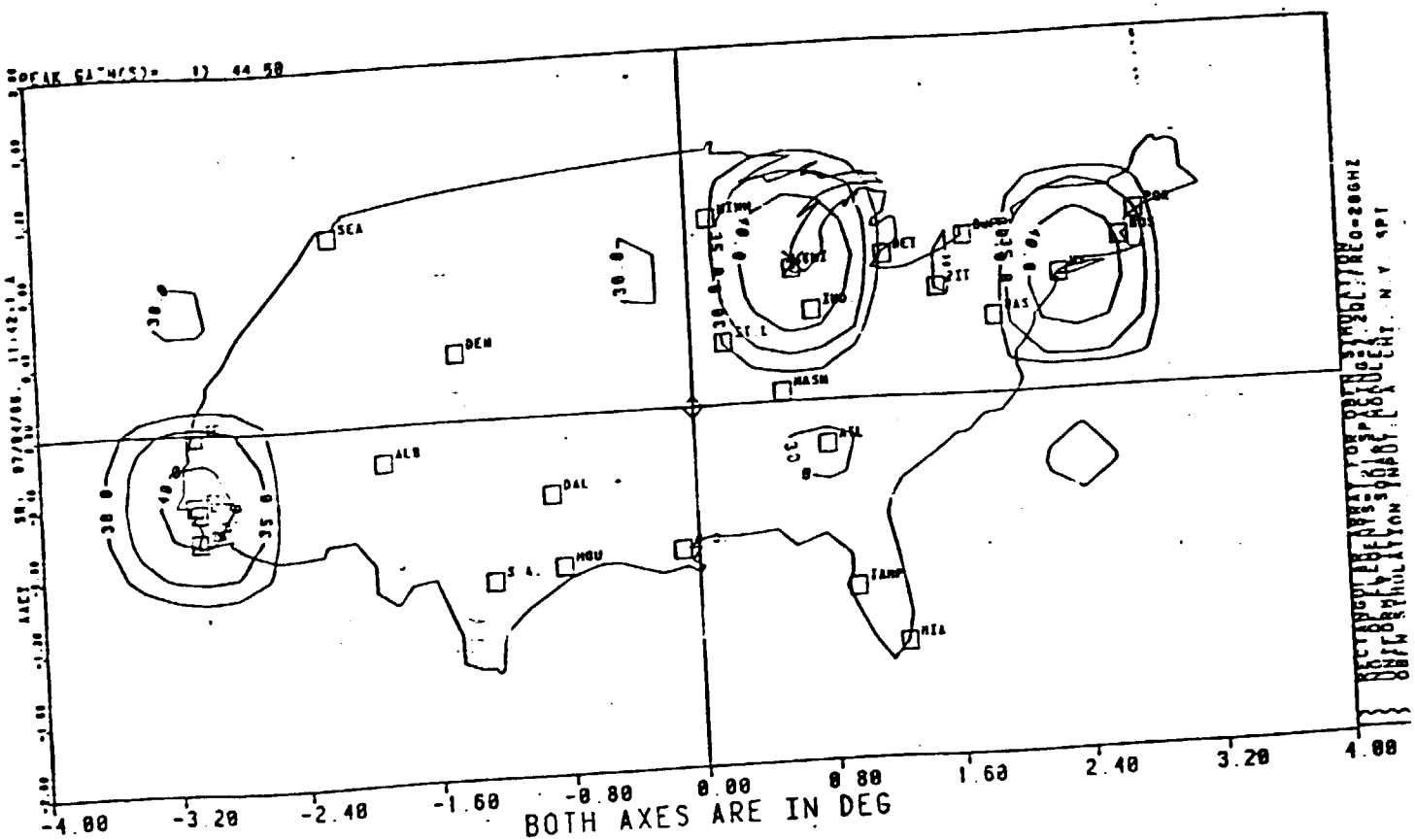

LOS ANGELES CHICAGO NEW YORK

FIGURE 2.6 MULTIPLE SPOT COVERAGE BEAMS

ideal LCLV with pixel transmittance varying between 1 and 0 (infinite contrast ratio). In reality, there is always some leakage through the light valve so that transmittance cannot go to zero. The effect of such leakage tends to broaden the main lobe and highten the sidelobe levels of the microwave far field pattern. A parametric study was thus conducted to determine the lower limit of contrast ratio for adequate far field patterns to result. Criteria for evaluation were sidelobe level and main lobe beamwidth. It was determined that for the network under study that a minimum contrast ratio of 30 dB was required for spot beams and a 25 dB level for sector beams before a 10% increase in sidelobe level or half power beamwidth (as applicable) was observed. The effect of a finite contrast ratio can be seen in Figure 2.7a and 2.7b which shows how the CONUS beam is affected by a 25 dB ratio. Note that Figure 2.7a details the main lobe and Figure 2.7b depicts the sidelobe structure. Sidelobe levels remain unchanged although some small main lobe perturbations occur.

Only a few case studies were performed during this investigation, although the computer model can be used to determine requirements of components such as the LCLV. Some suggestions for studies would be leakage between pixel electrodes, contrast ratio effects for other beam shapes and effects of fiber optic misalignments.

CONTRAST RATIO = ∞

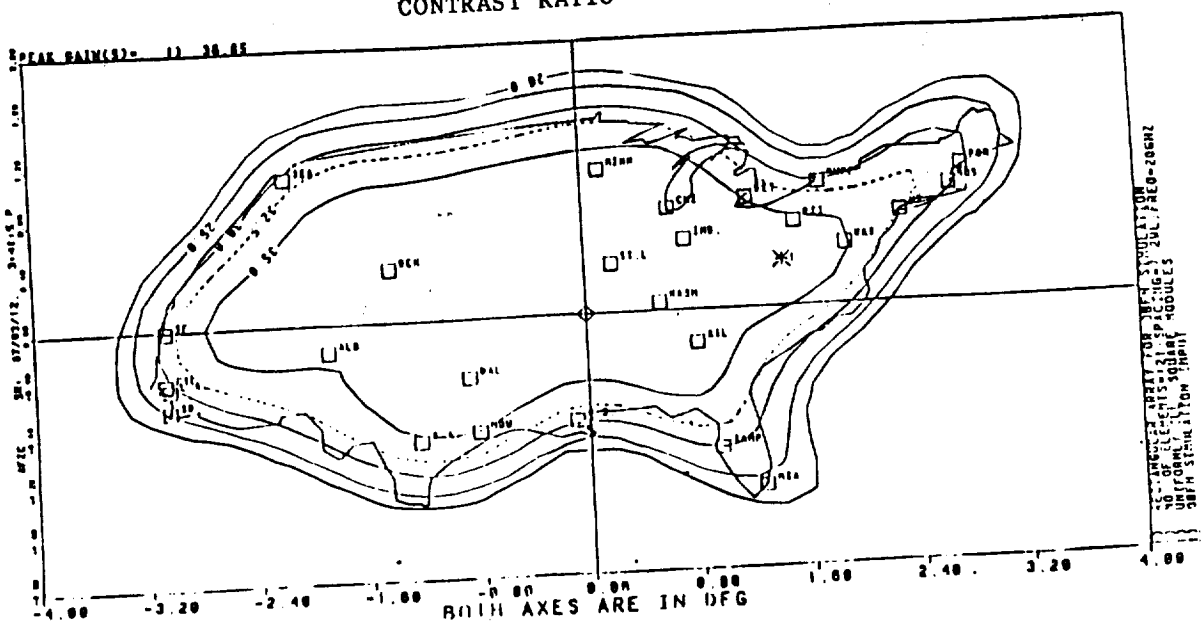

CONTRAST RATIO = 25dB

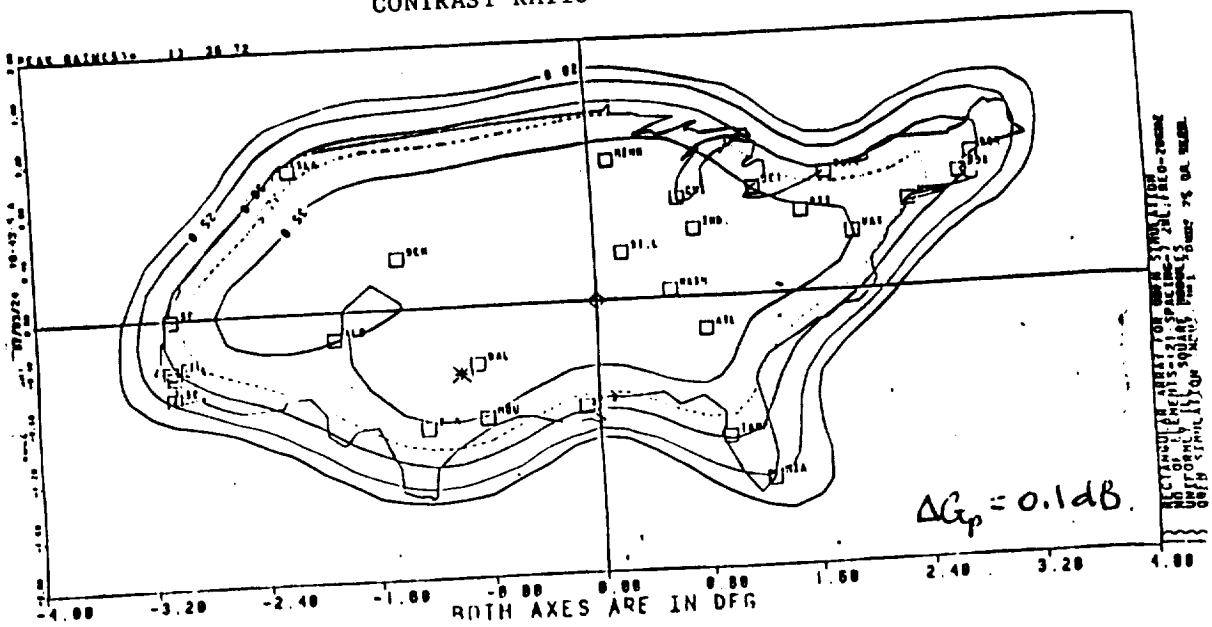

FIGURE 2.7a EFFECT OF ADJACENT PIXEL LEAKAGE ON FAR FIELD BEAM (MAIN LOBE)

CONTRAST RATIO = ∞

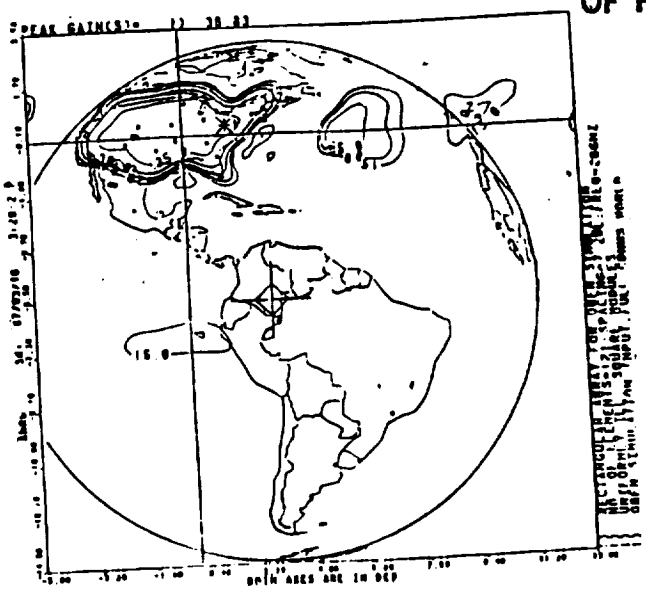

CONTRAST RATIO = 25dB

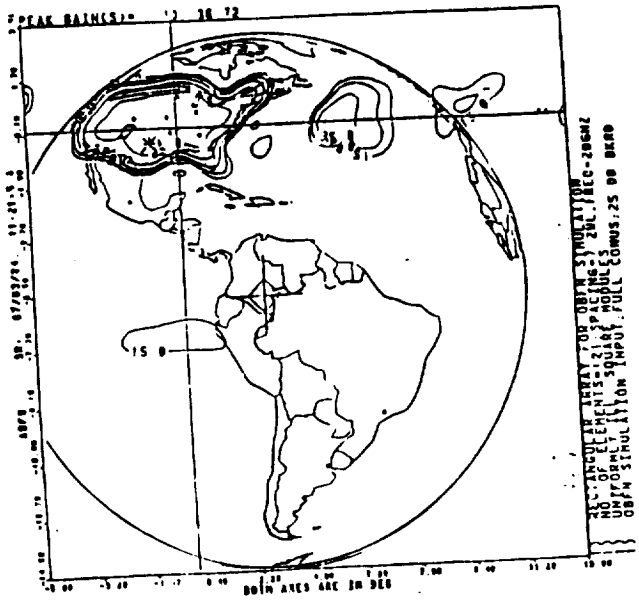

FIGURE 2.7b EFFECT OF ADJACENT PIXEL LEAKAGE ON FAR FIELD BEAM (SIDELOBES)

2.1 ERROR ANALYSIS

A coherent optical processor based beamforming network using the Fourier transform property of a lens is critically dependent upon the quality of the optical transform at the output plane. Errors due to imperfections in the optics, malfocused conditions, etc. will tend to degrade the production of an exact Fourier transform of the optical image at the processor output. Here a twofold approach is proposed to quantify and thus analyze the effects of such errors on beamforming performance.

Errors and their effect on the optical Fourier transform can be expressed in two basic canonical categories

1. Deterministic
2. Statistical

Previous studies[11] have made an attempt at classifying deterministic errors due to optimal path differences in the lens/collimator portion of the network. The approach examines the departure in the quality of the focused spot from ideal at the Fourier transform plane (i.e. output). Proper design of the collimation optics can hold to a minimum the effects of source amplitude taper at the output. Thus, we are concerned chiefly with phase errors in the wavefront at the transform plane. Analysis of such effects on the quality of the resultant microwave far field pattern can be accomplished by modification of the Fourier transform integral to include a quadratic phase modulation as a description of the optical path differences in the system. Thus, the field distribution at the fiber array is now expressible in the form:

---

11. D. Casasent Op. Cit.

$$E(x_2, y_2) = \frac{E_o}{j\lambda f} \sum_{n,m=1}^{N,M} t_{nm} e^{-j2\pi(b_n f_x + c_m f_y)} \times \iint_{A_p} e^{-j2\pi(x_1 f_x + y_1 f_y + Ax_1^2 + By_1^2)} dx_1\, dy_1 \quad (2.1.1)$$

here f_x and f_y are the spatial frequency components and bn, Cm are the phase offsets in the x and y planes respectively. The integration takes place over each individual pixels surface area A_p. Here, as in the unperturbed analysis, the pixel illumination function to (x,y) is constant over the pixel area varying as $0 \leq t_o \leq 1$. This form can now be coded into the OBFN analysis subroutine much in the same manner as the zero phase error case. The solution can be determined from standard Fresnel integrals.

The properties of the optical transform spatial frequency distribution must also be preserved at the microwave array aperture. The sampled spectrum at the fiber bundle interface must travel down each respective fiber optic transmission line, be downconverted and amplified for radiation from each array element. Random fluctuations in the amplitude and phase of the transform distribution at the antenna aperture could be attributable to several factors in the process of transmission to and downconversion at the interface. For example, the effect of temperature variations could physically alter fiber optic transmission line lengths creating phase fluctuations at the aperture.

Detector/amplifier nonlinearities could also contribute to amplitude and phase distortion in the aperture distribution. To achieve a first order quantization of these effects or antenna far field pattern performance, a statistical perturbation analysis is suggested. The two variables present at the aperture amplitude and phase can be modeled as independent random processes. The probability density

functions can be assumed to be uniform, with bounds determined by namelist inputs from the user. A parametric tolerance study could thus be conducted using this subroutine to determine network sensitivities to temperature, mechanical stresses, etc. using far field pattern degradation as a criteria.

3.0 TEMPORAL ANALYSIS

The preservation of signal quality in the microwave communications link is of great concern in the utilization of optical processor based beamforming networks. Thus it would be judicious to examine the impact of the processor scheme on signal parameters. These parameters include processor losses, signal to noise ratio, noise figure and processor dynamic range. This will serve to define the power requirements of the laser source to yield a specific signal quality.

In order to model the effect of the processor network on the modulating microwave signal, two fundamental categories were addressed. First, signal quality at the output of the processor was considered. Here, two figures of merit were chosen to quantify the performance, these being (1) network equivalent noise figure and (2) noise processes over and above the fundamental shot noise limit of the laser. Second, network laser power requirements were established as a function of desired signal to noise ratio at the output, number of array elements and modulation index of the modulating waveform. To examine the effect of the various components in the modulating path of the processor, it has been shown[12] that the optical link equations can be expressed as a cascaded noise figure model. The temporal link components such as the semiconductor laser and

12. Millimeter/Fiber Optic Links Op. Cit.

associated circuitry, external electroptic modulator and optical detector/preamplifier modules have had their individual parameters isolated by the model. The link model taken for the anaysis is shown in Figure 3.1. The input signal, S_{in} is amplified by an input preamplifier with gain and noise figure of G_1 and F_1 respectively. This is matched to the modulator impedance by a lossless matching network Z_1. The input signal is assumed to have a peak value, S_{inpk}, that must be accommodated by the modulator. Modulator and fiber optical losses, which include connector losses, coupling losses and propagation losses are represented as an overall loss H_M. The photodiode amplifier is assumed to have gain, G_2, and a noise figure F_2, and likewise the input is matched to the device by a lossless network Z_2.

The basic structure of the model now defined, an overall equivalent noise figure for the processor temporal path can be established. This can be defined by relating the network input and output signal to noise ratios and designated as F_{EQ} i.e.

$$F_{EQ} = \left(\frac{S}{N}\right)_{IN} / \left(\frac{S}{N}\right)_{OUT} \qquad (3.0.1)$$

The Friis formulation allows the modularization of noise figure into the individual components of the cascaded network (for n stages in cascade), thus

$$F_{EQ} = F_1 + \frac{F_2 - 1}{G_1} + \frac{F_3 - 1}{G_1 G_2} + \cdots \frac{F_n - 1}{G_1 G_2 \ldots G_{n-1}} \qquad (3.0.2)$$

Note that in the model depicted, noise contributions from the spatial processing path are considered to be of second order. Here the network can be considered as a two amplifier cascade with the addition of laser and photodiode shot noise power terms. The laser source contributes noise into the link independent of the

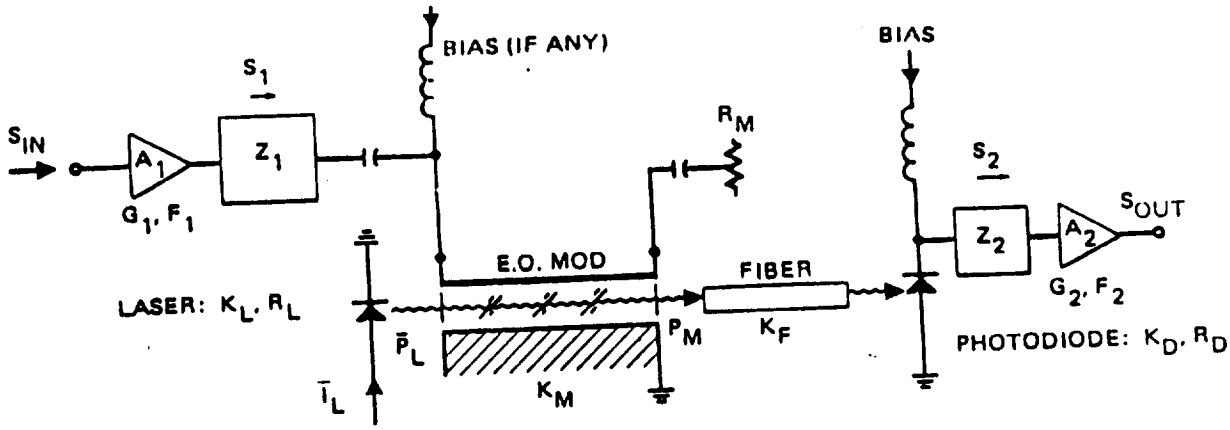

FIGURE 3.1 TEMPORAL PATH ANALYTIC MODEL

electroptic modulator, which is virtually noise free. These noise contributions can be reduced to three major processes, these being 1) Shot noise 2) Thermal noise and 3) Excess noise. The shot noise is a fundamental "lower limit" of noise power in semiconductor lasers. This noise results from the random nature of the electron recombinative process. Thermal noise is attributable to the active layer being at a finite temperature T. Excess noise is noise power contribution from processes other than previously mentioned and discussed shortly. The equivalent network noise figure can now be developed by accounting for each devices' noise contribution in the link. Thus, the output signal to noise ratio is found as

$$\left(\frac{S}{N}\right)_{OUT} = \frac{G_2 H_M^2 G_1 S_{in}}{G_2 H_M^2 G_1 F_1 KT\Delta f + G_2 H_M^2 \left(\frac{K_L}{R_m}\right)^2 S_{xn} + G_2 S_{dn} + G_2 (F_2 - 1) KT\Delta f}$$

Here the laser internal losses are represented by the transfer function K_L. The terms S_{xn} and S_{dn} are the equivalent noise powers in the source and detector respectively. Further refinement of the model allows the electroptic modulator to be assumed as a travelling wave interference type modulator (i.e. Mach-Zehnder). An optical intensity modulator of this type exhibits as the fraction of light transmitted across the applied voltage to be

$$\frac{I}{I_o} \sim \sin^2 \left\{ \frac{\pi V}{2 V_\pi} + \frac{\pi}{4} \right\}$$

where V_π is the "half-wave" voltage a parameter that takes into account the dimensions and material of the modulator which produces an 180^o optical phase shift. This particular type of modulator configuration has been chosen for its capabilities for utilization in the 20/30 GHz communications band as well as its

low power consumption. To further define our equation we recognize the following[13]

$$S_{inpk} = \frac{R_L (I_L - I_{tnr})^2}{G_1}$$

$$S_{xn} = 2 E_q I_L R_L \Delta f$$

$$S_{dn} = 2 q (I_L - I_{thr}) H_M \Delta f \sqrt{R_m R_D}$$

The resulting algebraic manipulation of the individual parameters of each device in the cascaded temporal path yields an expression for the final equivalent network noise figure

$$F_{EQ} = F_1 + \frac{2E}{G_1\left(\frac{KT}{q}\right)}\left[\frac{4V_\pi^2}{R_m}\frac{I_L}{(I_L - I_{thr})^2}\right] + \frac{2}{\chi}\sqrt{\frac{R_D}{Z_o}}\left[\frac{2\sqrt{QF_{EQ}KT\Delta f Z_o}}{H_{M1}\sqrt{G_1}\left(\frac{KT}{q}\right)}\right] + \frac{F_2 - 1}{H_{M1}^2 G_1} \quad (3.0.4)$$

The individual device variables used are defined as follows:

$F_1, F_2 =$	input, output amplifier noise figures
$G_1, G_2 =$	input, output amplifier gains
$I_L =$	laser current
$I_{thr} =$	laser threshold current
$R_m =$	modulator impedance
$x =$	percentage of peak voltage excursion V
$R_D =$	photodiode impedance
$R_L =$	laser impedance
$Z_o =$	interconnecting transmission time impedance
$H_M =$	temporal path losses
$K =$	Boltzman's constant
$T =$	ambient temperature
$q =$	electronic charge
$\Delta f =$	operating bandwidth

13. Ibid

The excess noise term E takes into account random intensity fluctuations greater than the shot noise associated with the bias current. This is dependent upon a number of material and structural parameters of the device. Additionally, conversion of laser phase noise to amplitude noise by dispersion in the link optical components can contribute to the excess noise process. Thus, this excess noise can be expressed as

$$E = \frac{i_{xn}^2}{2 q I_L \Delta f} \qquad (3.0.5)$$

where i_{xn}^2 is the equivalent mean square current fluctuation in the laser current that could produce an optical intensity fluctuation in the laser output. The denominator is just the expression for shot noise current. Thus, excess noise is just the ratio of mean square current fluctuations beyond shot noise to the fundamental lower limit of the noise mechanism in the semiconductor laser. The parameter Q expresses the dynamic range of the applied modulator drive signal i.e.

$$Q = \frac{S_{inpk}}{S_{inmin}} \qquad (3.0.6)$$

where

S_{inpk} = peak input drive signal power

S_{inmin} = minimum allowable drive signal power

The minimum signal allowable here is a signal that will yield a value of $(S/N)_{OUT}$ equal to unity. The equation for the equivalent noise figure can readily be seen to be a quadratic in terms of F_{EQ} with Q as a parameter. The input drive signal dynamic range Q can be related as a function of the network noise figure F_{EQ} with excess noise as a parameter. These relationships are shown in Figure 3.2. Network constants are set for small signal input inasmuch as distortion and resulting intermodulation products occur at high percentage modulation. These various network parameters are documented in tabular form in Table 3.1.1. An

TABLE 3.1.1

TEMPORAL PATH PARAMETERS (SMALL SIGNAL)

LINK PARAMETERS

$F_1 = F_2 = 1.5$ dB

$G_1 = G_2 = 40$ dB

$\Delta f = 20$ GHz

$T = 300^{\circ}K$

$Z_o = 50\Omega$

$H_M = -21$ dB

E/O MODULATOR

TYPE: $LiNbo_3$ TRAVELING WAVE

$V_\pi = 5V$

$X = 0.15$ (LINEAR REGION)

$R_{in} = 50\Omega$

LASER/PHOTODETECTOR PARAMETERS

$P_L = 10$ mW

$I_L = 40$ mA

$I_{thr} = 20$ mA

$R_D = 50\Omega$

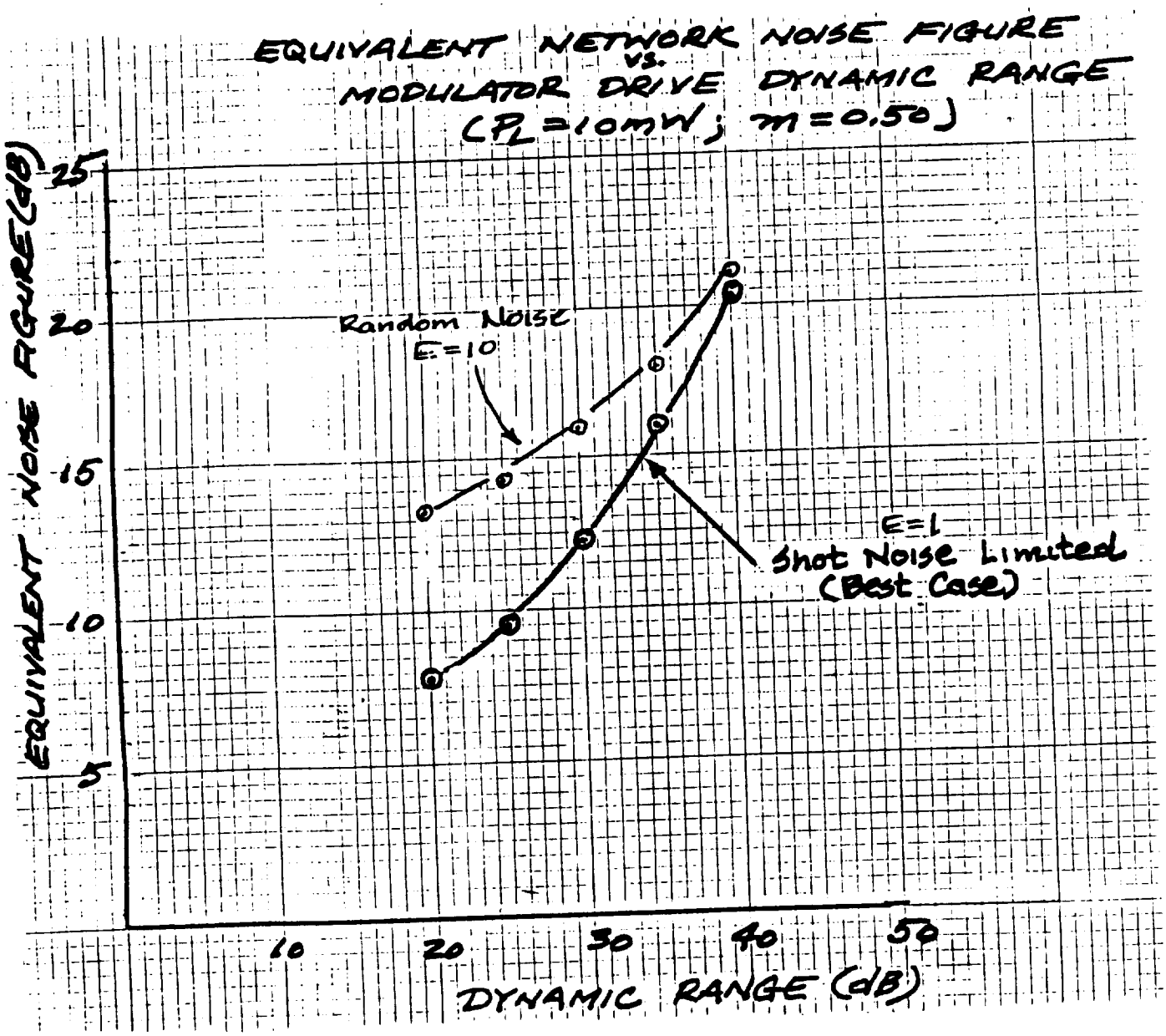

FIGURE 3.2 EQUIVALENT NETWORK NOISE FIGURE vs.

MODULATOR DRIVE DYNAMIC RANGE

arbitrary excess noise value of E=10 was chosen to compare to negligible excess noise at E=1. For a signal dynamic range of 20 dB, a 4-5 dB degradation in network noise figure results from a tenfold increase in excess system noise. Several factors have been examined in previous studies to help to improve the network noise figure. Choice of amplifier characteristics, modulator operating voltage and modulator impedance can be optimized for the best possible system operation. These aspects are cause for futher study.

The second prime issue of concern is the power requirements placed on the laser source. Here the signal quality must be preserved upon downconversion at the antenna aperture. The major figure of merit of signal quality is determined by its signal to noise ratio. Thus the laser power requirement will be directly accountable to the desired signal to noise ratio at the output of the processor. Since available source power will most likely be at a premium for space applications, a minimum power criteria was chosen for the analysis. Minimum power here is defined as the least power necessary to achieve reliable detection while maintaining a set signal to noise ratio over a given information bandwidth. Here the signal power was assumed to be low enough to be limited only by the thermal noise of the detector/amplifier modules at the antenna interface. Due to the fact that each array element must use a photodetector module, an expression for the required source power can be derived based on the minimum detectable signal at each element. Thus based on a broadband photodetection system without internal current gain, the required power can be expressible as[14] a function of output signal to noise ratio, i.e.

14. R.K. Cheo Fiber Optics Devices and Systems Prentice Hall 1985 Chapter 11

$$(P_R)_{min} = \frac{N_e h f_{op}}{m q \eta} \sqrt{\frac{8KT \Delta f}{R_D} \left(\frac{S}{N}\right)_o}$$

Here

R_D =	photodiode impedance
N_e =	number of array elments
h =	Planck's constant
f_{op} =	optical operating frequency
m =	modulation index
q =	electronic charge
η =	photodiode quantum efficiency
K =	Boltzman's constant
T =	ambient temperature
Δ f =	operating bandwidth
$\left(\frac{S}{N}\right)_o$ =	output signal to noise ratio

This now allows the investigation of output power required to achieve a desired signal to noise ratio of the signal at the output of the network. Figure 3.3 depicts these relationships using number of array elements and modulation index as parameters. It is immediately evident from the plots as well as intuitively that with increasing numbers of array elements, optical power requirements of the source increase. Modulation index (or depth of modulation) is also of importance here. This is due to the fact that at high percentage modulation distortion and intermodulation products result. It is seen, therefore, that a tradeoff exists between source power required and choice of modulation index. The lower the modulation index, the more optical power required in the network for a given array size. Theoretical results have been plotted for array sizes N_e = 100 and 1000 as well as 100% and 70% modulation.

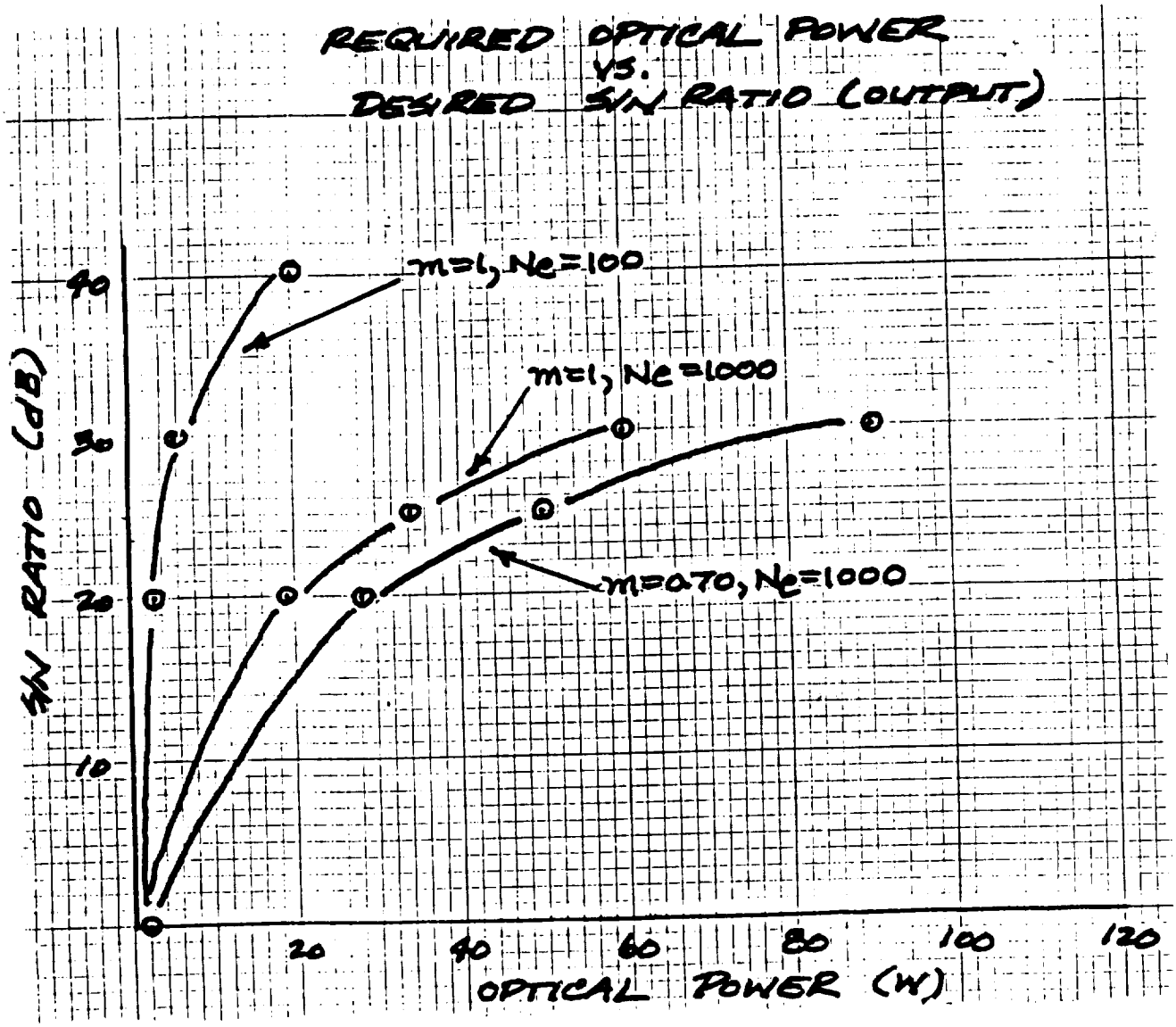

FIGURE 3.3 REQUIRED OPTICAL POWER vs.

DESIRED OUTPUT S/N RATIO

Another parameter of interest is network power conversion efficiency. Here each component or device in the network is assigned an optical power conversion efficiency index based on the absorbtion and/or reflection of optical power during the beamforming process.

Since parallel processing of both spatial and temporal aspects of the resultant antenna beam occurs in the network, the detected power at the output can be expressed as the sum of the individual paths:

Thus

$$P_D = (\eta_1 \cdot \eta_2 \cdots \eta_n) P_1 + (\eta_1 \cdot \eta_2 \cdots \eta_m) P_2 \qquad (3.0.8)$$

where

η = conversion efficiency index

P_1 = power in spatial path

P_2 = power in temporal path

To a first order, the principle components which contribute to optical power loss in the network are:

1) Spatial light modulator (Liquid Crystal Light Valve)
2) Electroptic temporal modulator
3) Fiber/Processor Coupling

The conversion efficiency of the spatial light modulator (in this case a liquid crystal light valve - LCLV) can be determined as the percentage of light reflected as compared to the incident collimated illumination i.e.

$$\eta_{LCLV} = \frac{(\text{Area of Pixel}) \times (\text{No. of Reflecting Pixels})}{(\text{Total Illuminated Area})} \qquad (3.0.9)$$

Here "pixel" denotes the individual control cells that comprise the surface of the light valve. As used in the beamforming network, the surface of the light valve represents the field of view over which the desired beam "footprint" will be formed. It is immediately evident that for a given field of view, the greater the reflecting area of the light valve surface and the better the optical conversion efficiency. Thus it will suffice to conclude that area coverage (i.e. sector beams) beams will be highly efficient whereas scanning spot beams with large scan angles will be inefficient. It would thus behove the designer to judiciously choose his light valve design such that his field of view is optimum.

The conversion efficiency of the electroptic temporal modulator can be reduced into two basic components, these being 1) imput/output coupling efficiency (i.e. interface VSWR) and 2) throughport loss (i.e. insertion loss). This can be described as

$$\eta_{11} = \eta_{22} = (1 - |\rho|^2)$$

where

ρ = modulus of reflection coefficient at input/output interfaces (assuming symmetry at interfaces).

and

$$\eta_{21} = 1 - \sqrt{\frac{P_o}{P_i}}$$

where

P_o = detected power

P_i = power input to modulator

Thus the total modulator conversion efficiency becomes

$$\eta_{MOD} = (1 - |\rho|^2)^2 \left(1 - \sqrt{\frac{P_o}{P_i}}\right) \qquad (3.0.10)$$

Finally, the coupling efficiency from the processor to the fiber optic bundle can be evaluated to a first order using Fresnel equations for the free space/dielectric interface. The design of the processor as described in Section 2.0 is addressed in such a manner as to hold the F.T. lens focal length to a value such that near normal incidence occurs at the interface. Additionally, the assumption is made that the fiber core diameter is many wavelengths, thus emulating a filled halfspace. Thus the coupling efficiency becomes

$$\eta_c = (1 - |\Gamma|^2) \frac{\text{Area of Fiber Core}}{\text{Total Fiber Area}} \qquad (3.0.11)$$

where $\Gamma = \dfrac{\sqrt{\epsilon_r} - \epsilon_r}{\sqrt{\epsilon_r} + \epsilon_r}$

and

ϵ_r = relative dielectric constant of fiber core

The total network power efficiency equation can now be formed. Note that the assumption is made that the effects due to losses in beam splitters, collimators, fiber interconnects and F.T. lens are of second order. Here the first order approximation for detected power becomes

$$P_D = (\eta_{MOD} \cdot \eta_c) P_1 + (\eta_{LCLV} \cdot \eta_c) P_2 \qquad (3.0.12)$$

For an equal power split in both processing paths and CONUS coverage (approximately $4^\circ x 7^\circ$ field of view) the network power conversion efficiency is on the order of 20%.

4.0 COMPONENT IDENTIFICATION

The realization of the optical processor based beamforming network into a breadboard configuration is the specific goal of this study. Therefore, the proper identification of key components in the network must be addressed. The selection of the devices to be used in the processor breadboard has been based on an anticipated usage in the 20/30 GHz communications band and outputs from the analysis model defining performance requirements. These criteria are then used as a basis for a trade-off study to determine exactly which devices are suitable to meet the specified requirements.

The critical components in the transmit configuration beamforming network are listed as follows:

1) Source (laser)
2) Spatial Light Modulator (SLM)
3) Temporal Modulator
4) Fiber Optic Transmission Lines
5) Photodetector/Amplifier Modules

All other components such as collimators, beam splitters and the Fourier transform lens are obtainable as off the shelf items and thus of no concern in the trade study. In order to adequately address each component's salient features and the rationale for their selection, each device will be described in individual subsections.

Sources - As described in Section 1.0 the processor requirement of a narrow linewidth, coherent source necessitates the selection of a device which exhibits these qualities. The most desireable choice for space based applications is most

logically a semiconductor laser. Unfortunately, due to the small resonant cavity that is characteristic of these devices, spontaneous emission occurs much more frequently, resulting in broadened spectral linewidths. For OBFN applications, (using coherent detection) the amount of tolerable broadening is only limited by the SLM, fiber and photodetector response bandwidths. The bandwidth characteristics of both devices are sufficient for reliable network operation, and will be described further in their individual sections.

The choice of the 1.3μm operating wavelength is twofold as mentioned in Section 1.0. Thus, the choice of an InGaAsP device is preferred for both operating wavelength and potential monolithic integration into an OBFN optical integrated circuit. Recent advances in InGaAsP device technology have yielded designs that can operate at λ_o = 1.3μm with linewidths as small as 3 nm.

SLM's - The current network software model has envisioned the utilization of a device based on the characteristics of the Hughes produced liquid crystal light valve as the spatial light modulator (SLM). The model assumes a two port device (as depicted in Figure 4.1) where an image incident on the CdS photoconductor modulates a coherent, monochromatic (laser) readout beam incident on the liquid crystal. The dielectric mirror reflects the readout light back through the liquid crystal and the light blocking layer aids in insuring the optical isolation of the two ports. On the readout side there is a quartz window, and on the writing side there is a fiber optic faceplate, which allows for lensless "imaging" of a CRT with a similar faceplate. It is envisioned that the entire writing side (from the fiber optic faceplate to the light blocking layer inclusive) of the valve could be eliminated; thus the direct electronic addressing of the electrode grid over the L.C. can be used for image creation. Current device configurations have pixel densities on the order of 813 pixels/inch, although the analytical model of the

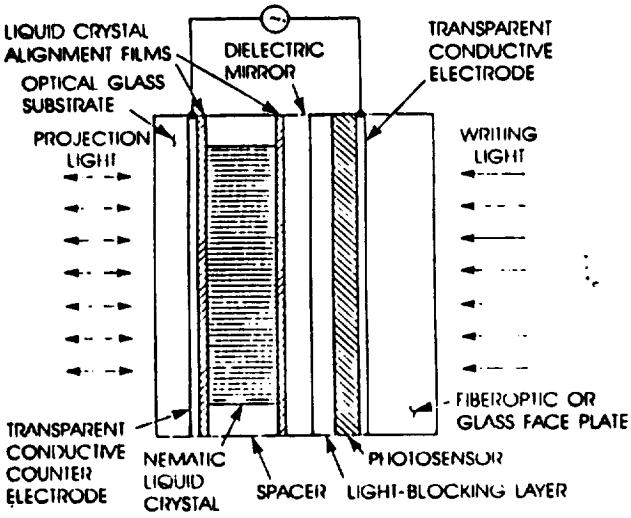

SIDE VIEW (CROSS SECTION)

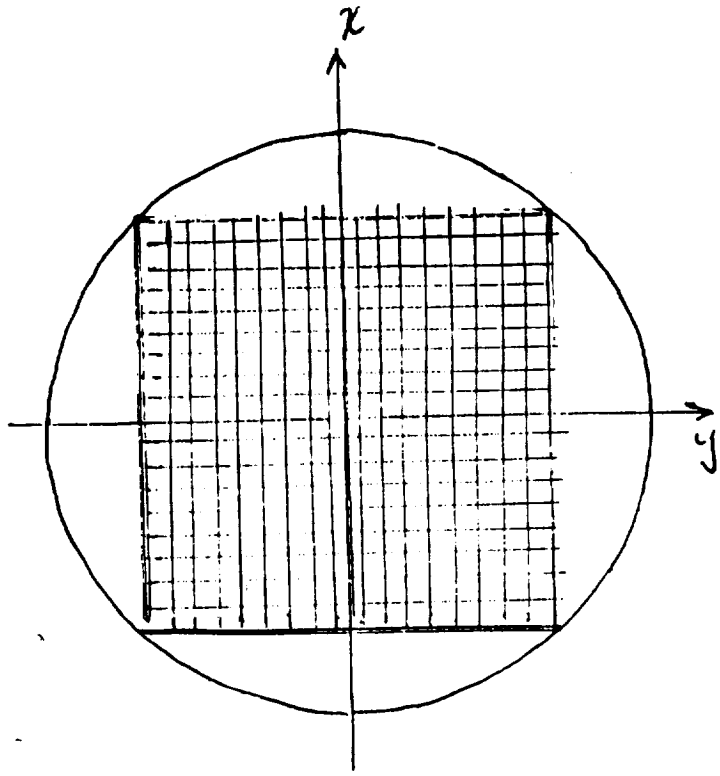

FRONT VIEW (FACING LASER LIGHT)

FIGURE 4.1 SPATIAL LIGHT MODULATOR

valve allows for this parameter to be input in accordance with the desired farfield pattern resolution to be produced. Additionally, current device technology has operational capability in the 450-650nm optical wavelength range. It is unknown at this point whether the currently used L.C.'s are operational at the desired 1.3 μm wavelength. If not, a new L.C. compound must be used for this wavelength. The remaining effort would be to redesign the dielectric mirror to operate at 1.3μm.

Temporal Modulators - External electroptic modulators have been selected for utilization in the optical processor network. The primary rationale for such devices is the fact that direct modulation of the laser diode source(s) is (are) not appropriate at the 20/30 GHz communications band[15]. A major disadvantage of the use of such external modulators is that the optical losses of the network are significantly increased due to coupling and propagation losses associated with these devices. This must be compensated for by higher source powers and judicious design of fiber/waveguide coupling devices.

The particular configuration of choice is the Mach-Zehnder interferometric modulator. This device is a traveling wave type modulator utilizing electroptic materials such as $LiNbO_3$ or GaAs as the substrate. This configuration was chosen over lumped element designs since for a given electrical drive power the traveling wave type is capable of achieving higher bandwidths for the same electrode design. What is desired of the ideal modulator is high energy efficiency, low modulation voltage and maximum bandwith. Recent advances in the state of the art have resulted in the publication of design procedures which address these issues[16]. Due to the fact that the optical-microwave dielectric constants being

15. "Millimeter/Fiber Optic Links" Op. Cit.

closer in GaAs than in $LiNbO_3$, GaAs modulators will have larger bandwidths than achievable through $LiNbO_3$ devices. In addition, since semiconductors enable more flexible electrode design, a higher electric field may be concentrated in the region of the optical waveguides. Thus, it would be wise to configure the modulators in GaAs in light of these reasons. Absorbtion type modulators based on the Franz-Keldysh effect have been eliminated as a potential candidate for consideration. Due to their poor transfer function characteristics, it is difficult to fabricate high speed analog modulators for the desired 20/30 GHz bandwidth.

Fiber Optic Transmission Lines - The two basic fiber optic transmission line types under consideration are (1) multimode and (2) single mode fibers. A multimode fiber propagates many modes as the name implies which gives rise to intermodal interference. This results in a limited bandwidth as a function of distance due to different propagation velocities of each individual mode down the length of the fiber. Current multimode fibers are limited to a bandwidth of approximately 1.5 GHz-Km of length. Thus 30 GHz bandwidth links would be cconstrained to under 40 meters in length. Single mode fibers, on the other hand, have the attribute that propagation distance is only limited by the group velocity dispersion of one single mode. The potential problem with utilization of single mode fibers though, is the very small size of the transmission line. For example, standard multimode fibers have core sizes of about 50μm in a 125 μm diameter fiber. By comparison, a single mode fiber used at 1.3μm has a core size of about 7μm; almost a magnitude smaller than multimode cores. A further complication arises because these very small cores must be aligned to within 0.5μm; less than one tenth the core diameter in order to achieve interconnection losses of less than 0.2 dB. For

16. Atsuki et al "Transmission Line aspects of the design of Broadband Electroptic Traveling Wave Modulators" IEEE LT5 No. 3 March 1987.

these reasons, it was decided to utilize multimode fibers inasmuch as spaceborne system will most likely have antenna/beamforming network separations under 40 meters.

Photodetector/Amplifier Modules - Operation in the 20/30 GHz frequency region wil require that both high speed photodetectors and GaAs FET amplifiers be integrated into a common optical receiver design. These receivers can be implemented as hybrid integrated circuits or as partially or fully monolithically integrated microwave circuits with the radiating antenna elements included. The advantage of the hybrid approach is that it can be implemented at 1.3 μm using heterotructure PIN InP/InGaAs detectors consisting of undoped InGaAs and transparent P type InP grown on n^+ InP substrates. The conceptual layout of the hybrid integrated receiver is shown in Figure 4.2. It consists of three main components; the detector chip, a quartz or alumina substrate with matching circuitry and the GaAs FET chip.

There appears to be substantial benefits from at least integrating the detector and matching circuitry onto the same chip in the event that the integrated receiver approach becomes a bit ambitious for initial studies. This requires the fabrication of a detector on a semi-insulating substrate; previous results by Wang et al[17] have indicated that this is possible. The primary advantages of this approach are that (1) the detector bond pad can be eliminated, which reduces the detector

17. Wang, et al "100 GHz Bandwidth Planar GaAs Photodiode" Electron Lett. Vol 19 P554-555 1983.

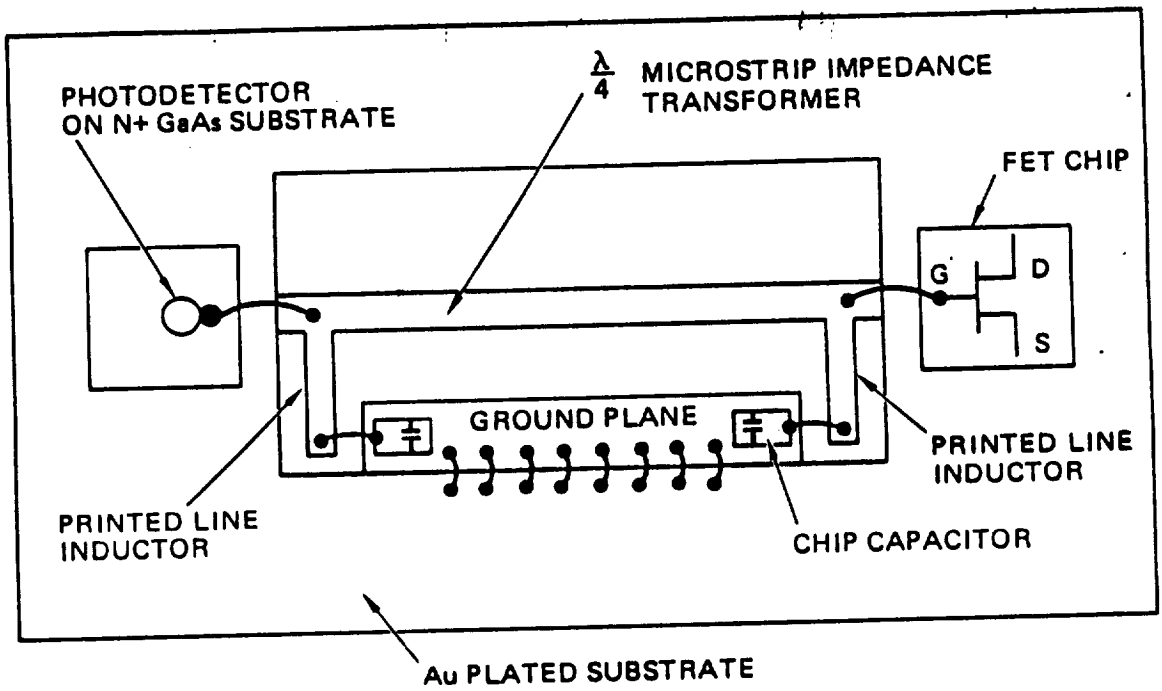

FIGURE 4.2 HYBRID INTEGRATED RECEIVER FOR OBFN

capacitance and (2) the number of bond wires required are reduced. Although inductors are desired in the receiver circuit, using bond wires to supply the inductance is much less precise than using printed lines on substrates.

Not considered in the temporal anaysis are photodetectors with internal gain. Such devices are termed as avalanche photodetectors. The photodetetors gain increases the receiver's sensitivity. This could allow for remote placement of the OBFN in relation to the radiating antenna aperture as well as lower required source power levels.

Rationale for the exclusion of such devices from consideration is based on the fact that shot noise generated in GaAs avalanche photo detectors is considerable. In this case, the avalanche photodiode detector may be only a little more sensitive than a good (low dark current) PIN heterostructure device followed by a low noise preamplifier. Thus the PIN photodetector should suffice for OBFN applications.

5.0 DISCUSSION

The feasibility of an optical procesor used for microwave antenna beamforming based on a liquid crystal light valve for image formation has been investigated. It has been established that a direct phase relationship exists between the optical phase in the processor at the fiber optic pickup and beam scanning in the far field. This is a design driver which determines inter-fiber spacing at the processor interface, and thus the practical aspect of selected designs.

Additionally, preliminary investigations into the amplitude relationships between the light valve created image, the Fourier image at the fiber interface (thus the antenna aperture distribution) and the resultant far field pattern were initiated. These studies were focused on the creation of generalized sector (i.e. area

coverage) beams for communications applications. It has been found that the synthesis of such beams are based on the superposition of individual sinc (x) sinc (y) functions (i.e. where sinc(u) = $\sin u / u$) at the fiber interface. This is due to the rectangular geometry chosen for the pixel control surfaces which comprise the image on the liquid crystal light valve. This technique is similar to the Woodward-Lawson sampling method, described in the literature[18]. A particular goal of interest in the creation of sector beams is direct control of the transition width at the edge of coverage. The transition width defines the level at which the main beam falls off into the sidelobe region. This is more commonly known as the main beam contour level. It has been determined that an increase in the spacial frequencies observed at the processor output will yield better resolution in the far field. This can be obtained either by (1) increase in the linear dimension of the pixel sizes or (2) increase in pixel grid density for a given field of view. Determination of the quantitative nature of this phenomenon must be found via parametric studies of these observations, a task yet to be undertaken. Sample beams have been created for CONUS coverage at a 10 dB edge of coverage contour through a trial and error procedure. This approach was then extended to quarter CONUS (i.e. Midwestern region) and multiple spot beam coverages.

The eventual goals of the beam forming studies in the spatial domain can be categorized into three main ideas:

1) Determination of Optimum LCLV Geometry - This includes determination of optimum pixel shape (i.e. circular, rectangular) as well as grid geometry (i.e. triangular, rectangular).

18. Stutzman et al Antenna Theory and Design Chapter 10 Wiley, 1982

2) Spatial Path Synthesis - Establish mathematical relationship between the nature of discritized image formation, aperture spatial filtering and far field beam formation.

3) Antenna Aperture Geometry - Determine impact of fiber/antenna element array geometry (i.e. lattice type) an aperture spatial filtering.

Once these objectives are met, complete control over optically formed microwave beams will be attainable.

Temporal aspects of the analysis have been addressed in recent publications[19]. The process of identification of potential sources of signal degradation in the processor network is similar to approaches used in optical communications network analysis.

Since the model initially conceived was simplistic in nature, most second order effects on signal quality were ignored. Most prominent is the fiber optic/processor coupling assumption. It is envisioned to extend the analysis to include diffraction effects and spillover losses with and without microlens augmentation. Adequate modeling of this interface is critical inasmuch as received power at the photodetector is proportional to the square root of the output signal to noise ratio.

19. See for example: W.E. Stephens et al, Op. Cit.

6.0 CONCLUSION

The concept of optical processor based microwave antenna beamforming has been deemed feasible supported by the analysis presented herein. Advantages and disadvantages of the approach as referenced to more conventional designs have been highlighted to establish the validity of this technique.

A quantitative view of the processor characteristics at the output of the antenna was presented. This has included effects of the processor on transmitted signal quality as well as spatial aspects of the beamforming process. As a result, a generalized computer model has been established to aid in the processor designed procedure.

A recommended physical layout for a 1.3μm breadboard processor is presented on which the analysis is based. To facilitate the selection of an optimum design, a component/device survey was conducted. The survey consisted of (1) a search of existing technology (2) recommendations for "best" device(s) for network applications and (3) identification of areas of needed component development.

Refinement of the analytical model comprises the bulk of future work to be done. This includes the determination of processor configurations for receive applications.

APPENDIX A

EFFECT OF AMPLITUDE MODULATION UPON PROCESSOR BEAM DETECTION

The difficulties associated with utilization of dual source schemes for the production of the desired microwave radiation frequency have been addressed in Section 1.0. The choice of a single source scheme has thus become attractive. A particular drawback of this approach is the problem caused by direct amplitude modulation of the reference beam in the processor. This problem is the creation of a "negative angle" beam at the output of the processor upon detection. This only occurs, though, for scanned beams. As an example let us consider the case of balanced modulation of the reference beam. The microwave modulated optical field can be expressed by

$$E_r(t) \quad A \cos(\omega_m t)\cos(\omega_o t) \tag{A.1}$$

where

ω_m = microwave radial frequency

ω_o = optical radial frequency.

If the spatial frequency signal sampled at the i^{th} optical fiber in the optical fiber bundle is given by $E_S(t)$ where,

$$E_S(t) = A_i \cos(\omega_o t + \phi_i) \tag{A.2}$$

here

A_i = Amplitude at the i^{th} optical fiber

ϕ_i = Phase at the i^{th} optical fiber

The the output of a square law detector is a low pass filtered version of the sum of these signals squared. Thus, the detected fields can be found from:

$$E_D(t) = \left[E_r(t) + E_s(t)\right]^2 \tag{A.3}$$

$$= \left\{A \cos(\omega_m t)\cos(\omega_o t) + A_i \cos(\omega_o t + \phi_i)\right\}^2$$

Expanding this expression and excluding all D.C. and high frequency components yields

$$E_D(t) = C\left\{\cos(\omega_m t - \phi_i) + \cos(\omega_m t + \phi_i)\right\} \quad (A.4)$$

where C = amplitude constant.

The first term on the right hand side of A.4 generates the undesired "negative angle" beam. A solution to this problem is similar to single sideband techniques used in communication systems. For instance, if a second microwave modulated reference signal is created in phase quadrature, such a signal can be expressible as

$$E_Q(t) = A\sin(\omega_m t)\sin(\omega_b t) \quad (A.5)$$

this can now be added to Equation A.2 to yield a detected signal as an output of a square law detection:

$$\begin{aligned} E_D^Q(t) &= \left[E_Q(t) + E_S(t)\right]^2 \\ &= \left\{A\sin(\omega_m t)\sin(\omega_o t) + A_i\cos(\omega_o t + \phi_i)\right\}^2 \end{aligned} \quad (A.6)$$

Expanding A.6 and excluding all D.C. and high frequncy components yields

$$E_D^Q(t) = C\left\{\cos(\omega_m t + \phi_i) - \cos(\omega_m t - \phi_i)\right\} \quad (A.7)$$

The desired signal can now be obtained by summation of A.4 and A.7 i.e.

$$\begin{aligned} E_D^F(t) &= E_D(t) + E_D^Q(t) \\ &= C\cos(\omega_m t + \phi_i) \end{aligned}$$

which is the desired downconverted aperture distribution that preserves the correct amplitude and phase.

APPENDIX B

SCHEMATIC OF RECOMMENDED TRANSMIT BEAMFORMING NETWORK

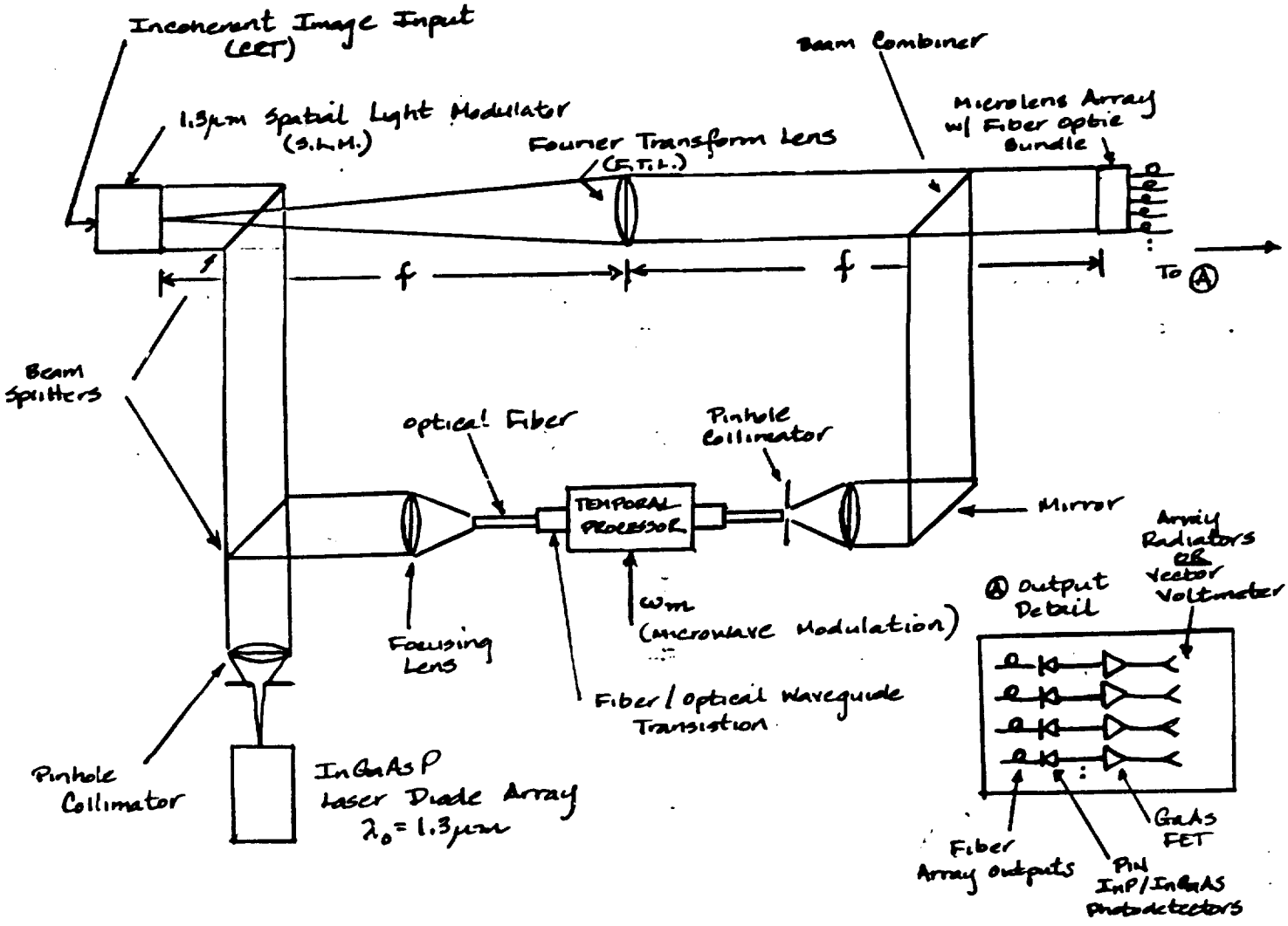

APPENDIX C

COMPUTER CODE FOR PROCESSOR SPATIAL PATH ANALYSIS

The source code listed has been designed specifically for LCLV diffraction from rectangular (square) pixel geometries. Thus, closed form functions (i.e. $\sin u/u$; $u = \pi x$) are used to determine the field distributions at the radiating aperture. Inputs describing the network geometry to be analyzed are provided via Data Statements. The source program and associated subroutines are coded in FORTRAN V and were exceucted on a CYBER 180 mini computer. All required inputs and outputs are designated via comment statements in the code. The example given is the input describing a full CONUS beam with a 25 dB leakage level emanating from the adjacent unused pixels.

This subroutine furnishes the complex aperture excitation coefficients (i.e. amplitude and phase) required for each individual array element to produce the desired far field beam. These coefficients must then be used in a conventional physical optics code for the prediction of the far field pattern performance. A flow chart detailing the individual steps involved in implementing the code is included for clarification.

OPTICAL PROCESSOR COMPUTER MODEL FLOW CHART

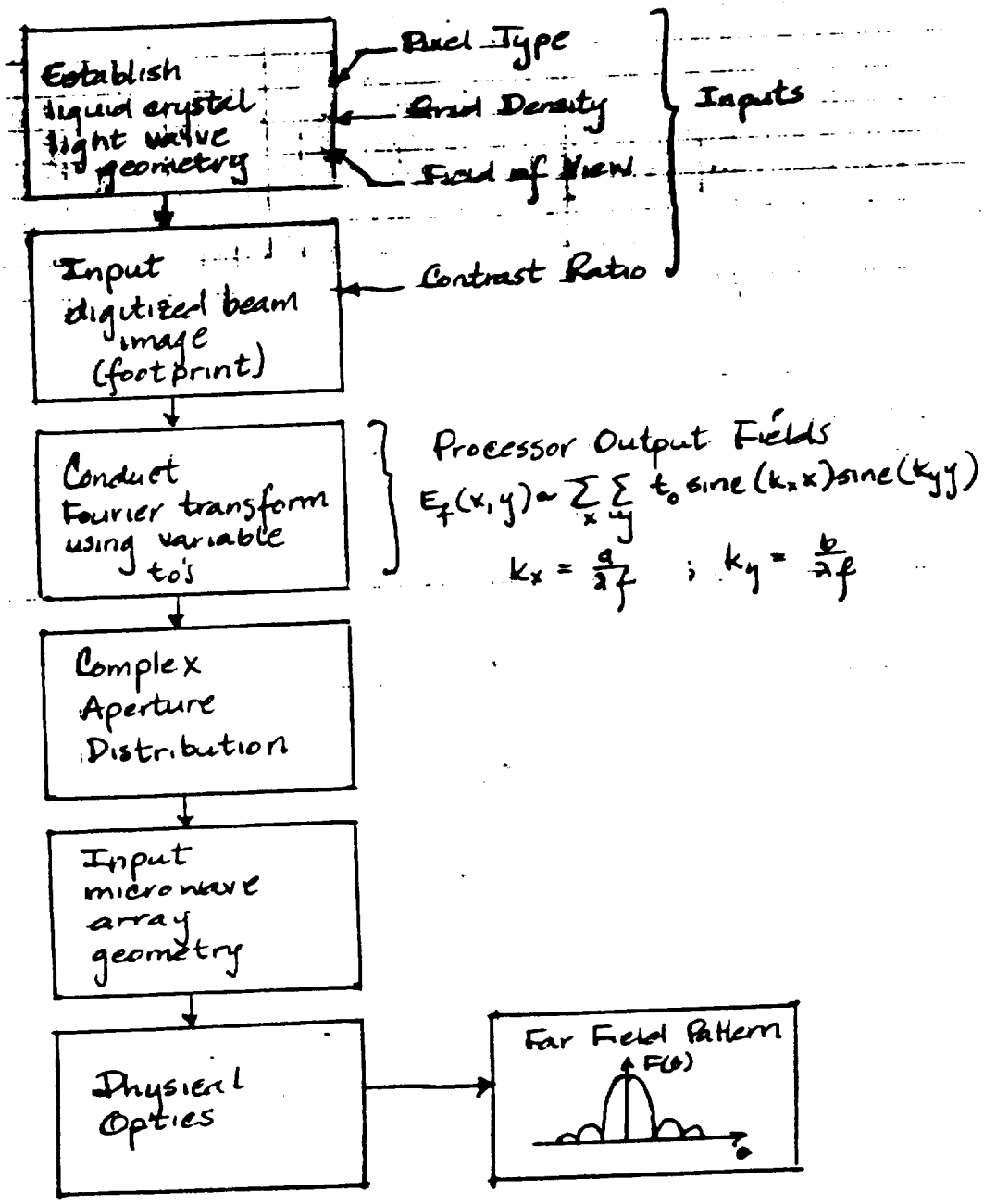

ORIGINAL PAGE IS
OF POOR QUALITY

```
LPA,T9999.ANTLAB1
/USER
*************************************************************************
*     HUGHES AIRCRAFT COMPANY - SPACE COMMUNICATIONS GROUP              *
*     ANTENNA SYSTEMS LABORATORY SOFTWARE                               *
*                                                                       *
*     PROPRIETARY INFORMATION -- THIS PROGRAM MAY NOT BE USED, COPIED   *
*     OR REPRODUCED, IN PART OR IN WHOLE, WITHOUT THE PRIOR WRITTEN     *
*     CONSENT OF HUGHES AIRCRAFT COMPANY.                               *
*************************************************************************
*                                                                       *
*     TITLE: MICROWAVE BEAMFORMING W/OPTICAL PROCESSOR                  *
*                                                                       *
*     APPLICATION: SIMULATE ANT. APERTURE EXCITATION                    *
*                                                                       *
*     AUTHOR(S): L.P. ANDERSON;F. BOLDISSAR                             *
*                                                                       *
*     TECHNICAL AUTHORITY: L.P.ANDERSON                                 *
*                                                                       *
*     IDENT. NUMBER: 002                   CREATION DATE: 2/87          *
*                                                                       *
*************************************************************************
*     REVISION LOG:                                                     *
*                                                                       *
*     REV #       DATE       MODIFIED BY          DESCRIPTION           *
*      1.  02/25/87  L.ANDERSON DESIGN FOR 1/4 CONUS                    *
*      2.03/11/87     PL.ANDERSON FULL CONUS(250B)   51X23 PIXEL ARRAY  *
*      3.                                                               *
*                                                                       *
*************************************************************************
FTN5.
LGO.
 READ.ROUTER
/FOR
      PROGRAM OBENS(INPUT,OUTPUT,TAPE5=INPUT,TAPE6=OUTPUT)
C
C  THIS PROGRAM COMPUTES THE INCIDENT FIELDS(AMP,PHZ)
C  ON A FIBER BUNDLE ARRAY. THE SOURCE OF THE FIELD
C  IS A LIGHT VALVE MODELED AS A LINEAR ARRAY OF
C  EQUALLY SPACED PIXELS.THE SOURCE FIELDS UNDERGO
C  A FOURIER TRANSFORMATION UPON TRANSMISSION THROUGH
C  A LENS;THE VALVE BEING IN THE INPUT FOCAL PLANE
C  AND THE FIBER BUNDLE BEING IN THE OUTPUT FOCAL PLANE.
C  THE OUTPUT FIELDS ARE THEN USED IN SR ..S A DISCRETE ..
C  APERTURE EXCITATION FOR A LINEAR ARRAY OF RADIATORS.
C
C
C  (THIS VERSION COMPUTES TWO DIMENSIONAL REPRESENTATION)
C   (MODIFIED VERSION ALLOWS FOR RECT.GRID IN L.V./FIBER ARA
C   ENHANCED RESOLUTION LEV FOR CONUS COVERAGE.
C   51X23 ARRAY PIXSZ=2.13E-4M.
C
      REAL  (51,23),EPWR(11,11),EPHZ(11,11)
      COMPLEX J,EFLD
      COMMON EXCITE/NFIBX,NFIBY,RELPWR(11,11),PHZ(11,11)
C
C  INPUT VARIABLES:NPIXX,NPIXY=#PIXELS ON L.V. IN X,Y
C                  PIXSP=PIXEL SPACING
C                  PIXSZ=PIXEL SIZE
C                  NFIBX,NFIBY=#FIBERS IN OUTPUT ARRAY IN
C                  FIBSP=FIBER/FIBER SPACING
C                  WL=OPERATING WAVELENGTH(OPTICAL)
C
```

```
C                    T=L.V. PIXEL TRANSMITTANCE
C
C
C
C  INPUT AND INITIALIZATION
C
      DATA NFIXA,NFIXY,PIXSP,PIXSZ/51,23,2.13E-4,4.13E-4/
      DATA NFIBX,NFIBY,FIBSP/11,11,102.E-6/
      DATA WL,PI/1.3E-6,3.1.9/
      DATA O/0.,1./
      PI=4.*ATAN(1.)
      FWHMA=0.
      FDIAX=(NFIBX-1)*FIBSP
      FDIAY=(NFIBY-1)*FIBSP
C
C  SET ALL PIXELS TO 25 DB TRANSMITTANCE
C
      DO 5 IPIX=1,NPIXA
      DO 5 JPIX=1,NPIXA
    5 T(IPIX,JPIX)=0.05**2
C
C  TURN ON DESIRED PIXELS FOR CONES
C
      DO 20 I=17,42
      DO 200 L=
  200 T(I,L)=1
C
C  BLOCK #2
C
      DO 201 I=43,4
      DO 201 L=
  201 T(I,L)=1
C
C  BLOCK #3
C
      DO 202 I=11,1
      DO 202 L=1,1
  202 T(I,L)=1
C
C  BLOCK #4
C
      DO 203 I=
      DO 203 L=18,20
  203 T(I,L)=1
C
C  BLOCK #5
C
      DO 204 I=17,1
      DO 204 L=4,
  204 T(I,L)=1
C
C  BLOCK #6
C
      DO 205 I=12,18
      DO 205 L=4,8
  205 T(I,L)=1
C
C  BLOCK #7
C
      DO 206 I=32,40
      DO 206 L=5,6
  206 T(I,L)=1
C
C  BLOCK #8
C
      DO 207 I=47,4
      DO 207 L=8,13
```

```
      207 T(I,L)=1
C
C  BLOCK #9
C
      DO 208 I=20,29
  208 T(I,5)=1
C
C  BLOCK #10
C
      DO 209 I=26,31
  209 T(I,6)=1
C
C  BLOCK #11
C
      DO 210 I=30,36
  210 T(I,2)=1
C
C  BLOCK #12
C
      DO 211 I=34,37
  211 T(I,3)=1
C
C  BLOCK #13
C
      DO 212 I=36,37
  212 T(I,4)=1
C
C  BLOCK #14
C
      DO 213 L=9,11
  213 T(50,L)=1
C
C  BLOCK #15
C
      DO 214 L=14,15
  214 T(48,L)=1
C
C  BLOCK #16
C
      DO 215 L=14,15
  215 T(47,L)=1
C
C  BLOCK #17
C
      DO 216 L=18,20
  216 T(46,L)=1
C
C  BLOCK #18
C
      DO 217 L=16,17
  217 T(44,L)=1
C
C  BLOCK #19
C
      DO 218 I=17,38
  218 T(I,22)=1
C
C  BLOCK #20
C
      DO 219 I=22,40
  219 T(I,23)=1
C
C  BLOCK #21
C
      DO 220 I=11,13
  220 T(K,19)=1
```

ORIGINAL PAGE IS
OF POOR QUALITY

```
C
C  BLOCK #22
C
      DO 221 I=13,17
  221 T(I,11)=1
C
C  BLOCK #23
C
      DO 222 I=14,16
  222 T(I,10)=1
C
C  BLOCK #24
C
      DO 223 I=9,10
  223 T(I,16)=1
C
C  BLOCK #25
C
      DO 224 I=8,10
  224 T(I,17)=1
C
C  BLOCK #26
C
      DO 225 I=8,9
  225 T(I,20)=1
C
C  BLOCK #27
C
      DO 226 I=1,8
  226 T(I,21)=1
C
C  BLOCK #28
C
      DO 227 I=8,9
  227 T(I,22)=1
C
C  BLOCK #29(1000 PIXELS)
C
      T(10,14)=1
      T(10,9)=1
      T(10,15)=1
      T(17,1)=1
      T(20,8)=1
      T(21,8)=1
      T(45,18)=1
C
C  FIXED FIELD COMPUTATION ...
C
      DO 20 IFIX=1,NFIXX
      XA=(FOVAX/2.)-FIXSP*(IFIX-1)
      FX=X2/(WL*FL)
      DO 20 JFIX=1,NFIXY
      YA=(FOVAY/2.)-FIXSP*(JFIX-1)
      FY=Y2/(WL*FL)
      FOVAX=(NFIXX-1)*FIXSP
      FOVAY=(NFIXY-1)*FIXSP
      EFLD=(0.,0.)
      DO 10 IFIX=1,NFIXX
      X1=(FOVAX/2.)-FIXSP*(IFIX-1)
      DO 10 JFIX=1,NFIXY
      Y1=(FOVAY/2.)-FIXSP*(JFIX-1)
      EFLD=EFLD+T(IFIX,JFIX)*(FIXSZ**2)*SINC(FX*PIXSZ)
     1*SINC(FY*FIXSZ)*CEXP(-J*2*PI*(FX*X1+FY*Y1))
   10 CONTINUE
C
C  COMPUTE FIELD POWER AND PHASE
```

```
C
      EAMP=CABS(EFLD)
      EPHZ(IFIB,JFIB)=ATAN2(AIMAG(EFLD),REAL(EFLD))*180./PI
      EPWR(IFIB,JFIB)=(EAMP)**2
      IF (EPWR(IFIB,JFIB).GT.PWRMAX) PWRMAX=EPWR(IFIB,JFIB)
   20 CONTINUE
C
C  NORMALIZE POWER AND PRINT RESULTS
C
      WRITE (6,110)
      DO 50 K=1,NFIB
      DO 50 L=1,NFIB
      RELPWR(K,L)=EPWR(K,L)/PWRMAX
      X2MM=((FDIAX/2.)-FIBSP*(K-1))*1000
      Y2MM=((FDIAY/2.)-FIBSP*(L-1))*1000
      WRITE(6,100)K,L,X2MM,Y2MM,RELPWR(K,L),EPHZ(K,L)
   50 CONTINUE
      STOP
  100 FORMAT (5X,I4,2X,I4,F7.2,5X,F7.2,5X,E8.2,5X,F6.1)
  110 FORMAT (  ,3X,'FIB NO  FIB POS(X),MM  FIB POS(Y),MM    INTEN
     1  PHZ' ,/)
      END
C
C  GENERATE SINC FUNCTION
C
      FUNCTION SINC(X)
      PI=4.*ATAN(1.)
      IF(ABS(X).GT.1.E-9)GO TO 30
      SINC=1.0
      GO TO 40
   30 SINC=SIN(X*PI)/(X*PI)
   40 RETURN
      END
/EOR
/EOF
```